

# QCD Factorization for $B \rightarrow \pi\pi\ell\nu$ Decays at Large Dipion Masses

Philipp Böer,<sup>1</sup> Thorsten Feldmann,<sup>2</sup> Danny van Dyk<sup>1,2</sup>

<sup>1</sup>*Theoretische Physik 1, Universität Siegen, Walter-Flex-Straße 3, D-57068 Siegen, Germany*

<sup>2</sup>*Physik-Institut, Universität Zürich, Winterthurerstrasse 190, CH-8057 Zürich, Switzerland*

*E-mail:* [boeer@physik.uni-siegen.de](mailto:boeer@physik.uni-siegen.de), [thorsten.feldmann@uni-siegen.de](mailto:thorsten.feldmann@uni-siegen.de),  
[dvandyk@physik.uzh.ch](mailto:dvandyk@physik.uzh.ch)

**ABSTRACT:** We introduce a factorization formula for semi-leptonic  $b \rightarrow u$  transitions in the exclusive decay mode  $B^- \rightarrow \pi^+\pi^-\ell^-\bar{\nu}_\ell$  in the limit of large pion energies and large dipion invariant mass. One contribution can be described in terms of a universal  $B \rightarrow \pi$  form factor and the convolution of a short-distance kernel  $T^{\text{I}}$  with the respective light-cone distribution amplitudes (LCDAs) of the positively charged pion. The second contribution, at leading power, completely factorizes, with a short-distance kernel  $T^{\text{II}}$  convoluted with the leading-twist LCDAs for both pions and the  $B$ -meson. We calculate the leading contributions to the short-distance kernels  $T^{\text{I}}$  and  $T^{\text{II}}$  in fixed-order perturbation theory, and discuss the approximate relations among the resulting  $B \rightarrow \pi\pi$  partial-wave form factors. Our results provide useful theoretical constraints for phenomenological models that aim to analyze the complete  $B \rightarrow \pi\pi\ell\nu$  phase space.

**KEYWORDS:** Heavy Quark Physics, QCD Factorization Theorems, Flavour Physics

---

<sup>1</sup>March 30, 2017. Siegen: SI-HEP-2016-05, QFET-2016-02; Zurich: ZU-TH 19/16; EOS-2016-04

---

## Contents

<b>1</b>	<b>Motivation</b>	<b>2</b>
<b>2</b>	<b>Kinematics and Power Counting</b>	<b>3</b>
<b>3</b>	<b>Factorization Formula</b>	<b>5</b>
3.1	The kernel $T^{\text{I}}$	6
3.2	The kernel $T^{\text{II}}$	11
<b>4</b>	<b><math>B \rightarrow \pi\pi</math> Form Factors and Observables</b>	<b>16</b>
4.1	Reduction of independent form factors in the QCDF limit	16
4.2	Numerical results	18
<b>5</b>	<b>Summary</b>	<b>25</b>
<b>A</b>	<b>Definition of Dipion Form Factors</b>	<b>26</b>
<b>B</b>	<b>Detailed Calculation for Kernel <math>T^{\text{II}}</math></b>	<b>27</b>
B.1	Recapitulation: the $B \rightarrow \pi$ form factor $f_+$	28
B.2	Expressions for $b \rightarrow d\pi^+ g\ell^- \bar{\nu}_\ell$ amplitudes	28
B.3	Contributions to $B \rightarrow \pi\pi$ matrix elements	31
<b>C</b>	<b>More on Kinematics</b>	<b>34</b>

---

# 1 Motivation

Exclusive charmless  $B$ -meson decays play an important role for the phenomenological analysis of quark flavour transitions in the Standard Model (SM) or its possible new-physics (NP) extensions (see e.g. the reviews in [1–5]). On the theoretical side, a systematic separation of short-distance effects in Quantum Chromodynamics (QCD) and long-distance hadronic physics can (at least partially) be achieved by utilizing an expansion in inverse powers of the large  $b$ -quark mass, i.e.  $\Lambda/m_b \ll 1$ , where  $\Lambda$  is a typical hadronic scale,  $\Lambda \lesssim 1$  GeV. In particular, this can be used to derive factorization formulas that allow one to implement QCD radiative corrections to the “naive” factorization approximation on a field-theoretical basis.

Factorization theorems for charmless nonleptonic  $B$ -meson decays into two mesons have been established at leading power in the heavy-mass expansion [6, 7]. Higher-order perturbative corrections have been calculated in [8–11] and [12–15] (see also [16] for a brief overview). One of the main motivations in this context was to increase the precision of theoretical predictions or, at least, get a more reliable theoretical assessment of hadronic uncertainties, which cannot be described by simple quantities like decay constants or transition form factors; see e.g. the phenomenological analyses in [17, 18]. The energies of the light hadrons in exclusive  $B$ -meson decays are not extremely large and power corrections still provide a major source of hadronic uncertainties, which are difficult to estimate and thus obscure the NP sensitivity in exclusive  $B$ -meson decays (see e.g. [19–22]).

For transitions which are dominated by tree-level exchange of  $W$ -bosons in the SM, potential NP effects are expected to play a subdominant role. The non-leptonic case has been extensively studied in the past; see e.g. the recent discussion in [23] and references therein. In this work, we focus on the semileptonic decays  $B^- \rightarrow \pi^+ \pi^- \ell^- \bar{\nu}_\ell$ , which are induced by  $b \rightarrow u \ell^- \bar{\nu}_\ell$  transitions and, in the SM, only involve one effective operator containing the left-handed  $b \rightarrow u$  quark current. QCDF is expected to be applicable in the kinematic situation where, in the  $B$ -meson rest frame, both pions recoil against each other with large energies of order  $m_b/2$ . The theoretical description features elements known from the analysis of nonleptonic  $B \rightarrow \pi\pi$  decays as in [17, 18] and semileptonic  $B \rightarrow \pi\ell\nu$  decays [24] and leads to a very similar QCD factorization formula. The confirmation of this factorization formula by explicit calculation of the leading non-trivial contributions to the hard-scattering kernels is the main subject of this paper. However, we will not aim at a rigorous factorization proof within the context of Soft-Collinear Effective Theory [25, 26]; a discussion along the lines of [27, 28] is left for future work.

One advantage of the  $B \rightarrow \pi\pi\ell\nu$  decay compared to its non-leptonic counterpart  $B \rightarrow \pi\pi$  is its richer kinematic structure that opens the possibility to analyze the angular distribution in the 4-body final state. Similar angular analyses have also been successfully exploited in phenomenological studies for other multi-body decay modes like  $B \rightarrow K\pi\ell\ell$  [29–31],  $B_s \rightarrow K\pi\ell\nu$  [32, 33], and  $\Lambda_b \rightarrow N\pi\ell\ell$  [34]. In particular, in certain corners of the phase space one finds approximate form factor relations that lead to simple theoretical predictions in the limit  $m_b \rightarrow \infty$  [35]. As we will see, this will also be the case in the kinematic situation that we are considering in this work. It could thus be interesting to

interpolate between different phase-space regions in  $B \rightarrow \pi\pi\ell\nu$  decays, using the results of this work and others (see e.g. [36–38]). Our formalism can also be generalized to certain phase-space regions in multi-pion final states, as considered in [39].

Our paper is organized as follows. In the next section we start with a brief summary of the relevant kinematic variables and the power-counting scheme that underlies the QCD factorization formula for  $B^- \rightarrow \pi^+\pi^-\ell^-\bar{\nu}_\ell$  that will be investigated in Section 3. In that section, we give a detailed derivation of the leading contribution (i.e.  $\mathcal{O}(\alpha_s)$ ) to the kernel  $T^{\text{I}}$ , also including contributions from the twist-3 distribution amplitudes of the positively charged pion, which are formally of subleading power but numerically enhanced. Furthermore, we calculate the kernel  $T^{\text{II}}$ , which arises from spectator scattering. We identify the endpoint-divergent contributions, which will be shown to exactly match the corresponding terms that appear in the universal “soft”  $B \rightarrow \pi$  form factor. The remaining finite terms provide the “factorizable” corrections of order  $\alpha_s^2$  to the  $B \rightarrow \pi\pi$  form factors at large dipion mass. In Section 4 we discuss the phenomenological implications, on the one hand in terms of approximate relations between the individual  $B \rightarrow \pi\pi$  partial-wave form factors, and on the other hand in terms of numerical estimates for two observables: the integrated decay rate and the pionic forward-backward asymmetry, in bins of the invariant dilepton and dipion masses. We conclude with a brief summary in Section 5. Detailed information on our conventions for the definition of the dipion form factors, as well as on the calculation of the individual diagrams contributing to the kernel  $T^{\text{II}}$  are collected in two appendices.

## 2 Kinematics and Power Counting

We define the kinematics for the decay

$$B^-(p) \rightarrow \pi^+(k_1)\pi^-(k_2)\bar{\nu}_\ell(q_1)\ell^-(q_2)$$

following the conventions in [35]. In the kinematic regime that we are interested in, it is safe to neglect the pion mass compared to the large  $B$ -meson mass and pion energies at large hadronic recoil. We will therefore set  $M_\pi^2 \rightarrow 0$  throughout the paper. Defining the sums and differences of hadronic and leptonic momenta as

$$\begin{aligned} q &= q_1 + q_2, & k &= k_1 + k_2, \\ \bar{q} &= q_1 - q_2, & \bar{k} &= k_1 - k_2, \end{aligned} \tag{2.1}$$

the hadronic system can be described by three kinematic Lorentz invariants, which can be chosen as the momentum transfer  $q^2$ , the dipion invariant mass  $k^2$ , and the scalar product

$$q \cdot \bar{k} = \frac{\sqrt{\lambda}}{2} \cos \theta_\pi. \tag{2.2}$$

Here  $\theta_\pi$  refers to the polar angle of the  $\pi^+$  meson in the dipion rest frame, and

$$\lambda \equiv M_B^4 + q^4 + k^4 - 2(M_B^2 q^2 + M_B^2 k^2 + q^2 k^2) \tag{2.3}$$

is the Källén function. For the following discussion it is sometimes more convenient to use the independent variables

$$E_{1,2} \equiv \frac{p \cdot k_{1,2}}{M_B} = \frac{M_B^2 + k^2 - q^2 \pm \cos \theta_\pi \sqrt{\lambda}}{4M_B} \quad \text{and} \quad k^2, \quad (2.4)$$

where  $E_{1,2}$  denote the energies of the individual pions in the  $B$ -meson rest frame, with

$$q^2 = M_B^2 - 2M_B(E_1 + E_2) + k^2, \quad q \cdot \bar{k} = M_B(E_1 - E_2), \quad (2.5)$$

and

$$\lambda = 4M_B^2((E_1 + E_2)^2 - k^2). \quad (2.6)$$

The power counting that underlies the factorization formula, to be introduced below, follows from the requirements that:

- (i) The energies of both pions in the  $B$ -meson rest frame are large to allow for the factorization of soft modes in the  $B$ -meson and collinear modes in the pions,

$$E_{1,2} \gg \Lambda, \quad (2.7)$$

where  $\Lambda$  is a typical hadronic scale;

- (ii) The invariant mass of the dipion system  $k^2$  is large, in order to allow for the factorization of collinear modes in the two different pion directions:

$$k^2 \gg \Lambda^2. \quad (2.8)$$

Allowing for generic values of  $q^2$ ,  $k^2$  and  $|\cos \theta_\pi|$ , the minimal pion energy corresponds to

$$E_{1,2} \geq E_{\min}(q^2, k^2, |\cos \theta_\pi|) = \frac{M_B^2 + k^2 - q^2 - |\cos \theta_\pi| \sqrt{\lambda}}{4M_B}. \quad (2.9)$$

Criterion (i) is therefore fulfilled if  $E^{\min} \gg \Lambda$ . For a quantitative estimate, we also have to take into account that the ratio  $M_B/\Lambda$  is not extremely large, and thus choose the phase space boundaries carefully. A conservative benchmark case would be, for instance, to require  $E_{\min} = M_B/3 \simeq 1.76$  GeV. Without any additional cuts on  $|\cos \theta_\pi|$  and regardless of the value of  $q^2$ , this can be achieved by setting  $k_{\min}^2 = 2M_B^2/3$  (see App. C). This defines

$$\begin{aligned} \text{Scenario A: } k_{\min}^2 &= 2M_B^2/3 \simeq 18.6 \text{ GeV}^2 \\ \Rightarrow E_{\min} &= M_B/3 \simeq 1.76 \text{ GeV} \quad (\text{for } |\cos \theta_\pi| \leq 1). \end{aligned} \quad (2.10)$$

Notice that in this case one finds that  $|E_1 - E_2| \leq 0.9$  GeV, i.e. one is very close to the kinematic endpoint, where

$$k^2 \simeq (E_1 + E_2)^2 \sim M_B^2, \quad |E_1 - E_2| \sim \Lambda \ll M_B, \quad \sqrt{\lambda} \ll M_B^2.$$

For  $q^2 \rightarrow 0$  this includes the special case for the kinematics in non-leptonic  $B \rightarrow \pi\pi$  decays [6]. In a still reasonable benchmark scenario we allow for slightly smaller values of  $E_{\min}$ , which can be achieved (again for all values of  $q^2$  and  $|\cos \theta_\pi|$ ) by a somewhat relaxed bound on  $k^2$ , ending up with

$$\begin{aligned} \text{Scenario B: } k_{\min}^2 &= M_B^2/2 \simeq 13.9 \text{ GeV}^2, \\ \Rightarrow E_{\min} &= M_B/4 \simeq 1.32 \text{ GeV} \quad (\text{for } |\cos \theta_\pi| \leq 1). \end{aligned} \quad (2.11)$$

The range of  $k^2$  can be further extended by restricting the size of  $|\cos \theta_\pi|$ , which yields a non-trivial lower-bound on the size of  $k^2$ . For the case considered in the following, the bound reads

$$E_{\min} < \frac{\sqrt{a^2 - 1}}{2a} \sqrt{k_{\min}^2}, \quad (2.12)$$

where  $|\cos \theta| \leq 1/a$ . (Further details and the derivation of this bound are relegated to App. C.) Aiming, as an example, at a value  $k_{\min}^2 = M_B^2/4$  for an angular bound  $|\cos \theta_\pi| \leq 1/3$ , we obtain

$$\begin{aligned} \text{Scenario C: } k_{\min}^2 &= M_B^2/4 \simeq 7 \text{ GeV}^2, \quad |\cos \theta_\pi| \leq 1/3 \\ \Rightarrow E_{\min} &= \frac{1}{3\sqrt{2}} M_B \simeq 1.24 \text{ GeV}. \end{aligned} \quad (2.13)$$

This includes the so-called “mercedes-star” configuration in  $B \rightarrow 3\pi$  decays [39], for which  $E_1 = E_2 = M_B/3$ ,  $k^2 = M_B^2/3$  and  $\cos \theta_\pi = 0$ .

Note that in each scenario above, the maximal value of the momentum transfer is given by

$$q_{\max}^2 = (M_B - \sqrt{k_{\min}^2})^2,$$

such that

$$\frac{q_{\max}^2}{M_B^2} \simeq 0.03 \quad (\text{Scenario A}), \quad \frac{q_{\max}^2}{M_B^2} \simeq 0.09 \quad (\text{B}), \quad \frac{q_{\max}^2}{M_B^2} \simeq 0.25 \quad (\text{C}).$$

In the following, we will retain the entire  $q^2$ -dependence in the theoretical expressions. In Scenarios A and B, however, the numerical values of  $q^2$  are sufficiently small that one can approximate the results by only keeping the linear term of a Taylor expansion in  $\sqrt{q^2}/M_B$ .

### 3 Factorization Formula

In the limit where the two final-state pions in the  $B$ -meson rest frame move nearly back-to-back with large energy and large invariant mass, the hadronic matrix elements for generic  $b \rightarrow u$  currents in the SM or beyond are expected to factorize in a similar way as the hadronic matrix elements of 4-quark and chromomagnetic penguin operators appearing in non-leptonic  $B \rightarrow \pi\pi$  decays [6, 7]. The noticeable difference between the two cases stems from the fact that the perturbative expansion for the short-distance kernels in  $B \rightarrow \pi\pi\ell\nu$

requires at least one hard gluon exchange to generate the additional quark-antiquark pair ending up in the final-state pions. We thus introduce the following factorization formula

$$\begin{aligned}
& \langle \pi^+(k_1) \pi^-(k_2) | \bar{\psi}_u \Gamma \psi_b | B^-(p) \rangle \\
&= \frac{2\pi f_\pi}{k^2} \left\{ \xi_\pi(E_2; \mu) \int_0^1 du \phi_\pi(u; \mu) T_\Gamma^I(u, k^2, E_1, E_2; \mu) \right. \\
&\quad + \frac{\pi^2 f_B f_\pi M_B}{N_C E_2^2} \int_0^1 du \int_0^1 dv \int_0^\infty \frac{d\omega}{\omega} \\
&\quad \times \phi_\pi(u; \mu) \phi_\pi(v; \mu) \phi_B^+(\omega; \mu) T_\Gamma^{II}(u, v, \omega, k^2, E_1, E_2; \mu) \Big\} \\
&\quad + \text{power corrections} .
\end{aligned} \tag{3.1}$$

In the first term,  $\xi_\pi(E_2)$  denotes the universal non-factorizable (“soft”)  $B^- \rightarrow \pi^-$  form factor in SCET [24, 26, 27], which can be defined as

$$\langle \pi^-(k_2) | \bar{\xi}^{(u)} \Gamma_X h_v^{(b)} | B(v) \rangle = \xi_\pi(E_2) \text{tr} [k_2 \Gamma_X P_v] . \tag{3.2}$$

Here

$$P_v \equiv \frac{\not{v} + M_B}{2M_B} \simeq \frac{1 + \not{v}_b}{2} \tag{3.3}$$

is the usual projector on the large components  $h_v^{(b)}$  of the heavy-quark spinor in Heavy-Quark Effective Theory (HQET) with the heavy-quark velocity  $v_b^\mu$ . Furthermore,  $\xi^{(u)}$  denotes the large component of an energetic up-quark spinor field in SCET. Finally,  $\phi_\pi(u)$  is the leading-twist LCDA of the (in this case positively charged) pion, and  $T_\Gamma^I$  denotes the short-distance kernel from hard gluon interactions with the constituents of the pions in the final state. The second term factorizes completely into leading-twist LCDAs,  $\phi_\pi$  and  $\phi_B$ , for the pions and the  $B$ -meson, convoluted with a short-distance kernel that contains the contributions from hard-collinear gluon exchange with the (would-be) spectator quark in the  $B$ -meson as well as additional hard-gluon corrections. (The normalization factors in (3.1) have been chosen for convenience.)

In the following, we are going to confirm this factorization structure by explicit calculation of the leading contributions to the kernels  $T^I$  and  $T^{II}$ .

### 3.1 The kernel $T^I$

The kernel  $T^I$  contains the short-distance QCD effects that *do not* involve the spectator quarks (and gluons) in the  $B$ -meson. The non-trivial tasks are then to show that

1. the leading-power contributions indeed only involve the leading-twist pion distribution amplitude of the  $\pi^+$  meson,
2. additional spectator interactions that would formally lead to endpoint-divergences in  $T^{II}$  are indeed universal and can be absorbed into the soft form factor  $\xi_\pi$ .

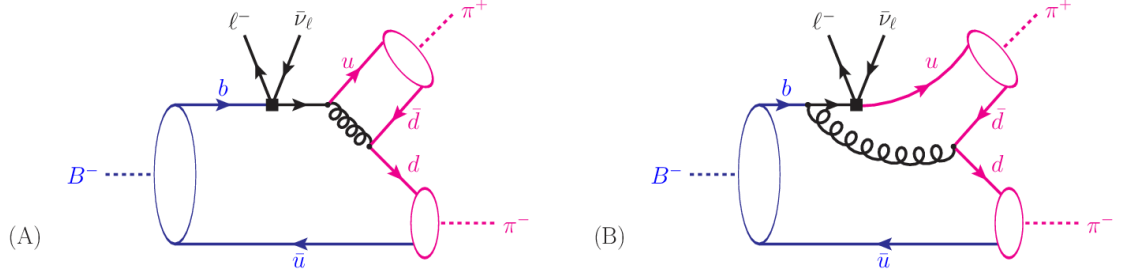


**Figure 1.** Sketch of QCD factorization in  $B^- \rightarrow \pi^+ \pi^- \ell^- \bar{\nu}_\ell$  decays at large dipion mass: Diagrams (i) and (ii) show the leading decay mechanism from hard gluon exchange. Radiative corrections, including factorizable and non-factorizable spectator interactions (see below) are not shown. (The colour coding refers to soft momentum modes in blue, and collinear momentum modes in magenta.)

We are going to address the first issue in this subsection by computing the leading amplitude term for the semi-partonic process  $b \rightarrow \pi^+ d \ell^- \bar{\nu}_\ell$ . The second problem is left for the next subsection when we discuss the leading spectator-scattering diagrams. We stress that, at this point, we are neither aiming at an all-order proof of the factorization formula, nor at its formal embedding into SCET.

At leading order in the strong-coupling constant, and projecting onto the 2-particle Fock state for the energetic pion, the process  $b \rightarrow \pi^+ d \ell^- \bar{\nu}_\ell$  is described by the two diagrams in Fig. 1. The leading-twist momentum space projector for the final-state pion (see e.g. [24]), reads

$$\mathcal{M}_{\pi^+}^{(2)}(u) = i f_\pi \frac{1}{N_C} \frac{\not{k}_1 \gamma_5}{4} \phi_\pi(u), \quad [(k_1)^2 = 0] \quad (3.4)$$

where  $u$  and  $\bar{u} = 1 - u$  are the longitudinal momentum fractions of the quark and anti-quark in a 2-particle Fock state, i.e.

$$k_{q1}^\mu \simeq u k_1^\mu, \quad k_{\bar{q}1}^\mu \simeq \bar{u} k_1^\mu. \quad (3.5)$$

Using Eq. (3.4), one obtains for a generic Dirac matrix  $\Gamma$

$$\langle \pi^+(k_1) d(k_{q2}) | \bar{\psi}_u \Gamma \psi_b | b(p_b) \rangle = 4\pi\alpha_s C_F \int_0^1 du [\bar{u}(k_{q2}) \Gamma_X u(p_b)] \quad (3.6)$$

with

$$\Gamma_X = -\frac{\gamma_\alpha \mathcal{M}_{\pi^+}^{(2)}(u) \gamma^\alpha (\not{p}_b - \not{q}) \Gamma}{(p_b - q)^2 (p_b - q - u k_1)^2} - \frac{\gamma_\alpha \mathcal{M}_{\pi^+}^{(2)}(u) \Gamma (u \not{k}_1 + \not{q} + m_b) \gamma^\alpha}{[(u k_1 + q)^2 - m_b^2] (p_b - q - u k_1)^2}, \quad (3.7)$$

in Feynman gauge.<sup>1</sup> Here we have used momentum conservation to replace  $k_{q2}^\mu = p_b^\mu - q^\mu - k_1^\mu$ . In the heavy-quark limit, we can further approximate  $m_b \simeq M_B$ , and  $p_b^\mu \simeq p^\mu$ ,

<sup>1</sup>One should not confuse the momentum fractions  $u, \bar{u} = 1 - u$  with the on-shell Dirac spinors  $u(p), \bar{u}(p)$ .



such that the denominators of the propagators can be expressed in terms of the hadronic Lorentz invariants defined above,

$$\begin{aligned}(p_b - q)^2 &\simeq (p - q)^2 = k^2, \\ (p_b - q - uk_1)^2 &\simeq (k_2 + \bar{u}k_1)^2 = \bar{u}k^2, \\ (uk_1 + q)^2 - m_b^2 &\simeq (p - \bar{u}k_1 - k_2)^2 - M_B^2 = \bar{u}(k^2 - 2M_BE_1) - 2M_BE_2.\end{aligned}\quad (3.8)$$

Assuming the Feynman mechanism to work, i.e. all endpoint-divergences from hard-collinear spectator scattering can be absorbed into the universal form factor  $\xi_\pi$  (which will be shown by explicit calculation of  $T_\Gamma^{\text{II}}$  below), we can replace the semi-partonic amplitude (3.7) by the hadronic one via (3.2),

$$\langle \pi^+(k_1) \pi^-(k_2) | \bar{\psi}_u \Gamma \psi_b | B^-(p) \rangle = 4\pi\alpha_s C_F \xi_\pi(E_2) \int_0^1 du \text{tr} [k_2 \Gamma_X P_v]. \quad (3.9)$$

From this we can read off the LO contribution to the hard-scattering kernel for a given Dirac structure  $\Gamma$ . For the presentation of the results, we find it convenient to define a basis of Dirac traces,<sup>2</sup>

$$\begin{aligned}s_1 &\equiv \text{tr}[k_1 \gamma_5 \Gamma P_v], & s_2 &\equiv \text{tr}[k_2 \gamma_5 \Gamma P_v], \\ s_3 &\equiv \text{tr}[k_1 \gamma_5 \Gamma], & s_4 &\equiv \text{tr}[k_2 \gamma_5 \Gamma], \\ s_5 &\equiv \frac{1}{M_B} \text{tr}[k_2 k_1 \gamma_5 \Gamma P_v], & s_6 &\equiv \frac{1}{M_B} \text{tr}[k_1 k_2 \gamma_5 \Gamma P_v], \\ s_7 &\equiv \frac{1}{M_B} \text{tr}[k_2 k_1 \gamma_5 \Gamma], & s_8 &\equiv \frac{1}{M_B} \text{tr}[k_1 k_2 \gamma_5 \Gamma].\end{aligned}\quad (3.10)$$

(Notice that in case of vector and axial-vector currents, one has  $s_3 = 2s_1$ ,  $s_4 = 2s_2$ , and  $s_7 = s_8 = 0$ .) In the LO expression for  $T_\Gamma^{\text{I}}$  following from (3.9) we find that only two independent functions of the quark momentum fraction  $u$  appear, which can be taken as<sup>3</sup>

$$f_1(u) \equiv \frac{-k^2}{\bar{u}(k^2 - 2E_1 M_B) - 2E_2 M_B}, \quad f_2(u) \equiv \frac{2E_2 M_B}{\bar{u} k^2} f_1(u). \quad (3.11)$$

The moment  $\langle \bar{u}^{-1} \rangle_\pi$  can be obtained from a linear combination,

$$\frac{1}{\bar{u}} = \left( \frac{2E_1 M_B}{k^2} - 1 \right) f_1(u) + f_2(u). \quad (3.12)$$

With these definitions we obtain

$$\begin{aligned}T_\Gamma^{\text{I}}(u, k^2, E_1, E_2) \Big|_{\text{LO}} &= i \frac{\alpha_s C_F}{N_C} \left\{ f_1(u) \left[ \left( \frac{2E_1 M_B}{k^2} - 1 \right) s_2 + \frac{1}{2} s_3 \right] \right. \\ &\quad \left. + f_2(u) \left[ s_1 + s_2 - \frac{M_B}{2E_2} s_5 - \frac{1}{2} s_7 \right] \right\} \\ &\equiv i \frac{\alpha_s C_F}{N_C} \frac{S_A + S_B^{(i)}(u) + S_B^{(ii)}(u)}{\bar{u}},\end{aligned}\quad (3.13)$$

<sup>2</sup>The corresponding structures without  $\gamma_5$  do not appear due to parity invariance of QCD.

<sup>3</sup>With this choice we obtain simple expressions in the limit  $k^2 \rightarrow 2E_1 M_B$ , namely  $f_1(u) \rightarrow E_1/E_2$  and  $f_2(u) \rightarrow 1/\bar{u}$ .

where, for later use, we have defined the abbreviations

$$S_A = s_2, \quad \frac{S_B^{(i)}(u)}{\bar{u}} = \frac{f_1(u)}{2} s_3 - \frac{M_B f_2(u)}{2E_2} s_5, \quad \frac{S_B^{(ii)}(u)}{\bar{u}} = f_2(u) \left[ s_1 - \frac{s_7}{2} \right]. \quad (3.14)$$

Notice that in the individual contributions to  $T_\Gamma^{\text{I}}$ , different projections of the Dirac matrix  $\Gamma$  in the original  $b \rightarrow u$  transition current appear. In particular, at LO, the hard-gluon exchange involves the “small” spinor components,  $(1 - P_v) \psi_b$  for the heavy quark (in the Dirac structures  $s_{3,7}$ ), and  $\frac{k_1 k_2}{k^2} \psi_u$  for the emitted  $u$ -quark (in the Dirac structures  $s_{2,6}$ ), but not both of them simultaneously (i.e. the structures  $s_4$  and  $s_8$  do not appear).

### 3.1.1 Twist-3 contributions

As is known from the QCDF analysis of  $B \rightarrow \pi\pi$  decays [7], twist-3 contributions to the hard-scattering kernels can be numerically important, despite the fact that they are formally power-suppressed. This can be traced back to a large numerical pre-factor,  $\mu_\pi = m_\pi^2/(m_u + m_d) \sim 2.5 \text{ GeV}$ , which is proportional to the quark condensate in QCD. The power corrections of the order  $\mu_\pi/\sqrt{k^2}$  will therefore be referred to as *chirally enhanced*. In addition, power corrections will potentially lead to non-factorizable contributions which show up as endpoint-divergent integrals in the perturbative calculation. In the computation of the kernel  $T_\Gamma^{\text{I}}$  the chirally-enhanced terms arise from the twist-3 two-particle LCDAs of the  $\pi^+$  meson. Here, a comment is in order about the definition of the transverse plane related to the underlying light-cone expansion for the *positively* charged pion state: As can be seen from the explicit structure of the LO diagrams leading to (3.7), the gluon propagator associated to the separation of the quark fields in the  $|\pi^+\rangle$  state involves the large momenta  $(p_b - q)^\mu \simeq (k_1^\mu + k_2^\mu)$  and  $k_1^\mu$ . The transverse momenta in the light-cone expansion for the  $\pi^+$  matrix elements are therefore to be chosen as transverse to both pion momenta,  $k_1$  and  $k_2$ . The parton momenta in the two-particle Fock state are then expanded as

$$\begin{aligned} \text{up-quark in } \pi^+: \quad & k_{q1}^\mu \simeq u k_1^\mu + k_\perp^\mu, \\ \text{anti-down-quark in } \pi^+: \quad & k_{\bar{q}1}^\mu \simeq \bar{u} k_1^\mu - k_\perp^\mu, \quad \text{with } k_{1,2} \cdot k_\perp \equiv 0, \end{aligned}$$

with  $|k_\perp|$  scaling as a hadronic momentum of order  $\Lambda$ . The corresponding twist-3 momentum-space projector can then be written as (see also [24])

$$\mathcal{M}_{\pi^+}^{(3)}(u) = \frac{i f_\pi \mu_\pi}{4} \frac{1}{N_C} \gamma_5 \left\{ -\phi_P(u) + i \sigma_{\mu\nu} \frac{k_1^\mu k_2^\nu}{k_1 \cdot k_2} \frac{\phi'_\sigma(u)}{6} - i \sigma_{\mu\nu} \frac{\phi_\sigma(u)}{6} k_1^\mu \frac{\partial}{\partial k_{\perp\nu}} \right\} \Big|_{k_\perp \rightarrow 0}. \quad (3.15)$$

Neglecting 3-particle contributions, the corresponding LCDAs are fixed by the equations of motion (see e.g. [40]),

$$\frac{u}{2} \left( \phi_P(u) + \frac{\phi'_\sigma(u)}{6} \right) \simeq \frac{\bar{u}}{2} \left( \phi_P(u) - \frac{\phi'_\sigma(u)}{6} \right) \simeq \frac{\phi_\sigma(u)}{6}, \quad (3.16)$$

leading to

$$\phi_P(u) \simeq 1, \quad \phi_\sigma(u) \simeq 6u\bar{u}. \quad (\text{“Wandzura-Wilczek approx.”}) \quad (3.17)$$

The twist-3 analogue to (3.7) can then be derived from

$$\Gamma_X \rightarrow -\frac{\gamma_\alpha \mathcal{M}_{\pi^+}^{(3)}(u) \gamma^\alpha (\not{p}_b - \not{q}) \Gamma}{(p_b - q)^2 (p_b - q - uk_1)^2} - \frac{\gamma_\alpha \mathcal{M}_{\pi^+}^{(3)}(u) \Gamma (uk_1 + \not{k}_\perp + \not{q} + m_b) \gamma^\alpha}{[(uk_1 + q)^2 + 2k_\perp \cdot q - m_b^2] (p_b - q - uk_1)^2}. \quad (3.18)$$

The corresponding contributions to the  $B \rightarrow \pi\pi$  matrix elements can be written as

$$\begin{aligned} & \langle \pi^+(k_1) \pi^-(k_2) | \bar{\psi}_u \Gamma \psi_b | B^-(p) \rangle \Big|_{\text{twist-3, LO}} \\ &= \frac{2\pi f_\pi}{k^2} \xi_\pi(E_2; \mu) \int_0^1 du \left( \phi_P(u) T_\Gamma^{(\text{I,P})}(u, k^2, E_1, E_2) + \phi_\sigma(u) T_\Gamma^{(\text{I},\sigma)}(u, k^2, E_1, E_2) \right). \end{aligned} \quad (3.19)$$

(Notice that – from the approximate relations in (3.17) – there is an ambiguity in expressing  $\phi'_\sigma(u)$  in terms of  $\phi_\sigma(u)$  and  $\phi_P(u)$ .) The first term in (3.18) contributes

$$T_\Gamma^{(\text{I,P})} = i \frac{\alpha_s C_F}{N_C} \frac{2M_B \mu_\pi}{k^2} \frac{s_5}{\bar{u}}. \quad (3.20)$$

The second term in (3.18) contributes

$$\begin{aligned} T_\Gamma^{(\text{I},\sigma)} &= i \frac{\alpha_s C_F}{N_C} \frac{M_B \mu_\pi}{3(\bar{u}(k^2 - 2M_B E_1) - 2M_B E_2)} \\ &\quad \times \left\{ \frac{1}{\bar{u}} \left[ -s_2 - \frac{E_2}{M_B} s_4 + \frac{2E_2 M_B}{k^2} s_6 + \frac{s_7}{2} \right] \right. \\ &\quad \left. + \frac{1}{u} \left[ -s_2 - \frac{E_2}{M_B} s_4 + \frac{2E_2 M_B}{k^2} s_6 + \frac{s_8}{2} \right] + \frac{2E_2 M_B}{k^2} \frac{s_5}{\bar{u}^2} \right\} \\ &\quad + i \frac{\alpha_s C_F}{N_C} \frac{2E_2 M_B^2 \mu_\pi}{3(\bar{u}(k^2 - 2M_B E_1) - 2M_B E_2)^2} \\ &\quad \times \left\{ \frac{1}{\bar{u}} \left[ \frac{E_2}{M_B} s_3 - s_5 + \frac{s_7}{2} + \frac{(4E_1 E_2 - k^2) M_B}{2E_2 k^2} s_5 \right] \right. \\ &\quad \left. - \left[ \frac{k^2}{2E_2 M_B} \left( s_1 - \frac{s_3}{2} \right) - \frac{E_1}{E_2} \frac{s_7}{2} \right] \right\}, \end{aligned} \quad (3.21)$$

where we have used the Wandzura-Wilczek approximation in (3.17). Notice that the potential endpoint divergence from the term  $\phi_P(u)/\bar{u}$  in the limit  $\bar{u} \rightarrow 0$  in (3.20) cancels with the last term in the first curly brackets in (3.21). This does not necessarily need to remain true after spectator-scattering corrections are taken into account, i.e. the contributions to the kernel  $T_\Gamma^{\text{II}}$  involving the twist-3 LCDAs of the positively charged pion can be expected to exhibit additional endpoint-divergent expressions, similar to what is observed in the QCDF approach to non-leptonic  $B \rightarrow \pi\pi$  decays. In the approximation (3.17) the convolution integrals with respect to the quark momentum fraction  $u$  can be done explicitly,

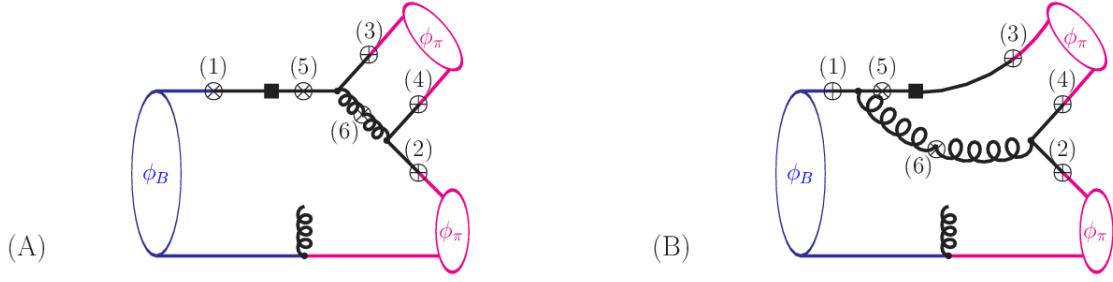


**Figure 2.** Diagrams contributing at LO to the kernel  $T^{\text{II}}$ . The hard-collinear gluon emitted from the lower quark line can be connected to any of the crosses numbered by (1 – 6).

leading to

$$\begin{aligned}
& \int_0^1 du \left( \phi_P(u) T_{\Gamma}^{(\text{I,P})}(u, k^2, E_1, E_2) + \phi_{\sigma}(u) T_{\Gamma}^{(\text{I},\sigma)}(u, k^2, E_1, E_2) \right) \\
& \simeq \frac{2M_B \mu_{\pi}}{k^2} \left( (1+L) s_5 - \frac{E_2}{E_1} L s_6 \right) \\
& - \frac{2M_B \mu_{\pi} L}{k^2 - 2M_B E_1} \left( s_2 + \frac{E_2}{M_B} s_4 - \frac{E_2}{E_1} s_6 \right) \\
& - \frac{2M_B \mu_{\pi}}{k^2 - 2M_B E_1} \left[ 1 + \frac{2M_B E_2}{k^2 - 2M_B E_1} L \right] \left( \frac{E_2}{M_B} s_3 - \frac{M_B}{2E_2} s_5 - \frac{s_8}{2} \right) \\
& + \frac{2M_B k^2 \mu_{\pi}}{(k^2 - 2M_B E_1)^2} \left[ 1 + \left( \frac{2M_B E_2}{k^2 - 2M_B E_1} - \frac{1}{2} \right) L \right] (2s_1 - s_3 - s_7) \quad (3.22)
\end{aligned}$$

with

$$L \equiv \ln \left[ \frac{2M_B E_1 + 2M_B E_2 - k^2}{2M_B E_2} \right] = \ln \left[ \frac{M_B^2 - q^2}{2M_B E_2} \right]. \quad (3.23)$$

Notice that the twist-3 contributions to  $T_{\Gamma}^{\text{I}}$  now also involve the Dirac structures  $s_{4,6,8}$  which did not appear in (3.14).

### 3.2 The kernel $T^{\text{II}}$

The leading contribution to the kernel  $T^{\text{II}}$  in the QCD factorization formula (3.1) arises from diagrams where – in addition to the hard-gluon process in Fig. 1 – a “hard-collinear” gluon connects to the (would-be) spectator quark in the  $B$ -meson. The relevant Feynman diagrams are summarized in Fig. 2, and will be discussed in turn in Appendix B.

Again, a comment is in order about the definition of the transverse plane, now related to the underlying light-cone expansion for the *negatively* charged pion state: In contrast to the situation discussed around (3.15) for the partonic kinematics in the  $|\pi^+\rangle$  state, the hard-collinear gluon propagator associated to the separation of the quark fields in the  $|\pi^-\rangle$  state involves the large momenta  $p_b^{\mu} \sim p^{\mu}$  and  $k_2^{\mu}$ . The transverse momenta in the light-cone expansion for the  $\pi^-$  matrix elements are therefore conveniently chosen as transverse

to  $p$  and  $k_2$ . The parton momenta in the two-particle Fock state are then expanded as

$$\begin{aligned} \text{down-quark in } \pi^-: \quad & k_{q2}^\mu \simeq v k_2^\mu + \bar{k}_\perp^\mu, \\ \text{anti-up-quark in } \pi^-: \quad & k_{\bar{q}2}^\mu \simeq \bar{v} k_2^\mu - \bar{k}_\perp^\mu, \quad \text{with } k_2 \cdot \bar{k}_\perp = p \cdot \bar{k}_\perp \equiv 0, \end{aligned}$$

with  $v$  ( $\bar{v} = 1 - v$ ) denoting the longitudinal momentum fraction of the quark (anti-quark), and  $|\bar{k}_\perp|$  scaling as a hadronic momentum of order  $\Lambda$ . The corresponding twist-3 momentum-space projector should then be written as

$$\mathcal{M}_{\pi^-}^{(3)}(v) = \frac{if_\pi \mu_\pi}{4} \frac{1}{N_C} \gamma_5 \left\{ -\phi_P(v) + i\sigma_{\mu\nu} \frac{k_2^\mu p^\nu}{p \cdot k_2} \frac{\phi'_\sigma(v)}{6} - i\sigma_{\mu\nu} \frac{\phi_\sigma(v)}{6} k_2^\mu \frac{\partial}{\partial \bar{k}_{\perp\nu}} \right\} \Big|_{\bar{k}_\perp \rightarrow 0}. \quad (3.24)$$

Neglecting 3-particle contributions, the corresponding LCDAs will again be fixed by the equations of motion as in (3.17).

With the same argument, we define the transverse momenta  $l_\perp$  of the light anti-quark in the  $B$ -meson, such that the momentum-space projector for the 2-particle distribution amplitudes can be written as in [24],

$$\mathcal{M}_B^{(WW)}(\omega) = -\frac{if_B M_B}{4} \frac{1}{N_C} \left[ P_v \left\{ \phi_B^+(\omega) \not{n}_+ + \phi_B^-(\omega) \left( \not{n}_- - \omega \gamma_\perp^\nu \frac{\partial}{\partial l_\perp^\nu} \right) \right\} \gamma_5 \right] \Big|_{l_\perp \rightarrow 0}, \quad (3.25)$$

where  $v_b^\mu = p^\mu/M_B$ ,  $n_-^\mu = k_2^\mu/(v_b \cdot k_2)$  and  $n_+^\mu = 2v_b^\mu - n_-^\mu$ , and  $\omega = (n_- \cdot l)$  is the light-cone projection of the light anti-quark momentum. As indicated, we again work in the Wandzura-Wilczek approximation and neglect the 3-particle DAs.

The individual contributions from a given diagram X to the  $B \rightarrow \pi\pi$  matrix element will be decomposed as follows,

$$\begin{aligned} & \langle \pi^+(k_1) \pi^-(k_2) | \bar{\psi}_u \Gamma \psi_b | B^-(p) \rangle \Big|_{(\text{Diagram X})} \\ &= \frac{2\pi f_\pi}{k^2} \frac{i\alpha_s^2 C_F}{4\pi N_C} \frac{\pi^2 f_B f_\pi M_B}{N_C E_2^2} \int_0^1 du \phi_\pi(u) \int_0^1 dv \int_0^\infty d\omega \left( g_{(X)}^{\text{finite}} + g_{(X)}^{\text{endpoint}} \right). \quad (3.26) \end{aligned}$$

Detailed inspection of the diagrams in Fig. 2 reveals that the corresponding contributions can be calculated in a similar way as the spectator-scattering contributions to the  $B \rightarrow \pi$  form factors considered in [24] at leading non-vanishing order. In particular, we find that all the endpoint-sensitive (formally divergent) contributions from 2-particle Fock states at leading power in the  $1/M_B$  expansion can be absorbed into the universal form factor  $\xi_\pi$ , with the definition of the associated hard kernel  $T_\Gamma^I$  derived in Eq. (3.14). The details of the calculation for the individual subdiagrams can be found in Appendix B.

### 3.2.1 Endpoint-divergent terms

In Table 1, we summarize the results for the endpoint-divergent terms as appearing in the individual diagrams when calculated in Feynman gauge. Here, we have introduced the additional abbreviations

$$-v_\perp^2 = \frac{4E_1 E_2}{k^2} - 1, \quad (3.27)$$

structure	A1	A2	A3 + A4	A5	A6	A1-A6
$\frac{2E_2 M_B}{\bar{u}^2 k^2} s_5 \frac{\phi_B^+(\omega)}{\omega} \frac{\phi_\pi(v)}{2v\bar{v}}$	0	0	$-C_{FA} 2v$	0	$C_A \frac{v-\bar{v}}{2}$	$2vC_F - \frac{C_A}{2}$
$\frac{S_A}{\bar{u}} \frac{\phi_B^-(\omega)}{\omega} \frac{\phi_\pi(v)}{\bar{v}^2}$	$C_F \frac{1}{v}$	$C_F \bar{v}$	$C_{FA} \frac{\bar{v}}{v}$	0	$-\frac{C_A}{2} \frac{\bar{v}}{v}$	$C_F (1 + \bar{v})$
$\frac{S_A}{\bar{u}} \frac{\phi_B^+(\omega)}{\omega} \frac{\mu_\pi \phi_\sigma(v)}{6\bar{v}^3 E_2}$	$C_F$	0	0	0	0	$C_F$
$2\mu_\pi \frac{S_A}{\bar{u}} \frac{\phi_B^+(\omega)}{\omega^2} \frac{\phi_P(v)}{\bar{v}}$	0	$C_F$	0	0	0	$C_F$

structure	B1	B2	B3+B5	B4	B6	B1-B6
$\frac{2E_2 M_B}{\bar{u}^2 k^2} s_5 \frac{\phi_B^+(\omega)}{\omega} \frac{\phi_\pi(v)}{2v\bar{v}}$	0	0	0	$C_{FA} 2v$	$C_A \frac{\bar{v}-v}{2}$	$\frac{C_A}{2} - 2vC_F$
$\frac{S_B^{(i)}}{\bar{u}} \frac{\phi_B^+(\omega)}{\omega} \frac{\phi_\pi(v)}{\bar{v}^2}$	0	0	$-C_{FA} v_\perp^2$	$C_{FA} v_\perp^2$	0	0
$\frac{S_B^{(i)} + S_B^{(ii)}}{\bar{u}} \frac{\phi_B^-(\omega)}{\omega} \frac{\phi_\pi(v)}{\bar{v}^2}$	$C_F \frac{1}{v}$	$C_F \bar{v}$	$C_{FA} \frac{1}{v}$	$-C_{FA}$	$-\frac{C_A}{2} \frac{\bar{v}}{v}$	$C_F (1 + \bar{v})$
$\frac{S_B^{(i)} + S_B^{(ii)}}{\bar{u}} \frac{\phi_B^+(\omega)}{\omega} \frac{\mu_\pi \phi_\sigma(v)}{6\bar{v}^3 E_2}$	$C_F$	0	$-C_{FA} v_\perp^2$	$C_{FA} v_\perp^2$	0	$C_F$
$\frac{S_B^{(i)}}{\bar{u}} \frac{\phi_B^-(\omega)}{\omega} \frac{\mu_\pi \phi_\sigma(v)}{6\bar{v}^3 E_2}$	0	0	$C_{FA} v_\perp^2$	$-C_{FA} v_\perp^2$	0	0
$2\mu_\pi \frac{S_B^{(i)} + S_B^{(ii)}}{\bar{u}} \frac{\phi_B^+(\omega)}{\omega^2} \frac{\phi_P(v)}{\bar{v}}$	0	$C_F$	0	0	0	$C_F$

**Table 1.** Endpoint-divergent contributions  $g_{(X)}^{\text{endpoint}}$  from diagrams (A1-A6) and (B1-B6) in Feynman gauge.

where  $v_\perp^\mu$  denotes the transverse components of the  $b$ -quark velocity with respect to the  $k_1$ - $k_2$  plane, and

$$C_{FA} = \frac{C_A}{2} - C_F = \frac{1}{2N_C}, \quad (3.28)$$

for the coefficient of the sub-leading colour structure. We further use Eq. (3.17) to replace

$$\frac{\mu_\pi}{2E_2} \left( \phi_P(v) - \frac{\phi'_\sigma(v)}{6} \right) \simeq \frac{\mu_\pi \phi_\sigma(v)}{6\bar{v}E_2}. \quad (3.29)$$

We observed that some obvious cancellations (of sometimes rather complicated structures) appear inbetween diagrams (A3,A4) and (B3,B5), respectively. For the sake of readability, we only show the combined results. The final expression for the endpoint-divergent terms arises as the result of rather non-trivial cancellations among the individual diagrams, see Table 1. This also involves the cancellation of endpoint-divergences related to the momentum fraction  $\bar{u} \rightarrow 0$  of the anti-quark in the *positively* charged pion, as expected from

colour-transparency arguments [6]. We obtain

$$\begin{aligned} & \langle \pi^+(k_1) \pi^-(k_2) | \bar{\psi}_u \Gamma \psi_b | B^-(p) \rangle \Big|_{(A1-A6, B1-B6)} \\ &= \frac{2\pi f_\pi \xi_\pi^{(\text{HSA})}(E_2)}{k^2} \int_0^1 du \phi_\pi(u) T_\Gamma^{\text{I}}(u, k^2, E_1, E_2) + \text{finite terms}, \end{aligned} \quad (3.30)$$

where the corresponding endpoint-divergent contributions in  $\xi_\pi^{(\text{HSA})}(E_2)$  have been calculated in [24] and can be found in Eq. (B.3) in the appendix. We thus recover the very same structures as in (3.13), confirming the assumptions that we made in the derivation of  $T_\Gamma^{\text{I}}$  in Section 3.1. Notice that in Feynman gauge all diagrams (except for A5) contribute, and the correct cancellation/combination of endpoint-divergences provides a useful cross-check of our calculation and a non-trivial aspect for the confirmation of the factorization hypothesis.

### 3.2.2 Finite Terms

The remaining (endpoint-finite) terms can then be associated to the kernel  $T_\Gamma^{\text{II}}$ , thus verifying the factorization formula (3.1) to leading order in the perturbative expansion.

**Large- $N_C$  limit:** Neglecting corrections that vanish in the limit  $N_C \rightarrow \infty$  (which amounts to setting  $C_A = 2C_F$ ), the hadronic information in the LO expression for  $T_\Gamma^{\text{II}}$  can be encoded in terms of the functions

$$\begin{aligned} f_3(u, v) &= \frac{\phi_\pi(v)}{\bar{u} v}, & f_4(u, v) &= \frac{\phi_\pi(v)}{\bar{u} v \bar{v}}, \\ f_5(u, v) &= \frac{4vE_2(k^2 - E_1M_B) + \bar{v}k^2M_B}{v\bar{v}k^2M_B} f_1(u), \\ f_6(u, v) &= \frac{4vE_2(k^2 - E_1M_B) + \bar{v}k^2M_B}{v\bar{v}k^2M_B} f_2(u). \end{aligned} \quad (3.31)$$

Notice that only three of these functions are linearly independent, since

$$\begin{aligned} & f_6(u, v) + \left( \frac{2E_1M_B}{k^2} - 1 \right) f_5(u, v) \\ & + \left( \frac{4E_1E_2}{k^2} - \frac{4E_2}{M_B} \right) f_4(u, v) - \left( 1 - \frac{4E_2}{M_B} + \frac{4E_1E_2}{k^2} \right) f_3(u, v) = 0. \end{aligned} \quad (3.32)$$

The explicit computation of the individual diagrams in Feynman gauge (see appendix B) yields

$$\begin{aligned} g_{(A1-A6)}^{\text{finite}} \Big|_{C_A=2C_F} &= C_F \left\{ f_3(u, v) \left( s_2 - \frac{2E_2M_B}{k^2} s_6 \right) \right. \\ & \quad \left. + f_4(u, v) \left( \frac{E_2}{M_B} s_4 + \frac{2E_2M_B}{k^2} s_5 \right) \right\} \frac{\phi_B^+(\omega)}{\omega}, \end{aligned} \quad (3.33)$$

and

$$g_{(B1-B6)}^{\text{finite}} \Big|_{C_A=2C_F} = C_F \left\{ -f_3(u, v) \frac{2E_2}{M_B} s_3 + f_4(u, v) \frac{E_2}{M_B} s_3 + f_5(u, v) \frac{s_3}{2} - f_6(u, v) \frac{M_B}{2E_2} s_5 \right\} \frac{\phi_B^+(\omega)}{\omega}. \quad (3.34)$$

As a consequence of (3.32), the results only depends on *three* new independent Dirac structures, which can be chosen as

$$\left[ s_2 + \frac{M_B(4E_1E_2 - k^2)}{2E_2k^2} s_5 - \frac{2E_2M_B}{k^2} s_6 \right], \quad \left[ s_3 - \frac{M_B(k^2 - 2E_1M_B)}{E_2k^2} s_5 \right], \quad \left[ s_4 - \frac{M_B(k^2 - 2E_2M_B)}{E_2k^2} s_5 \right].$$

**Subleading terms in  $1/N_C$ :** Including finite terms of order  $(\frac{C_A}{2} - C_F) = \frac{1}{2N_C}$ , which arise from the diagrams  $B_3$  and  $B_5$ , we encounter two more hadronic functions,

$$f_7(u, v) \equiv \frac{-2E_2M_B}{\bar{u}(vk^2 - 2E_1M_B) - 2vE_2M_B} f_4(u, v), \quad f_8(u, v) \equiv \frac{\bar{u}k^2(M_B - 2vE_2) + 4vE_2^2M_B}{2E_2(\bar{u}(k^2 - 2E_1M_B) - 2E_2M_B)} f_7(u, v), \quad (3.35)$$

entering as

$$g_{(B1-B6)}^{\text{finite}} \Big|_{\frac{C_A}{2}-C_F} = \left( \frac{C_A}{2} - C_F \right) \left\{ - (f_7(u, v) + f_8(u, v)) \frac{E_2}{M_B} \left[ s_3 - \frac{M_B(k^2 - 2E_1M_B)}{E_2k^2} s_5 \right] - f_7(u, v) \left[ \frac{s_7}{2} - \frac{M_B}{2E_2} s_5 \right] \right\} \frac{\phi_B^+(\omega)}{\omega}. \quad (3.36)$$

This involves another independent Dirac structure,  $\left[ \frac{s_7}{2} - \frac{M_B}{2E_2} s_5 \right]$ .

**Final result for  $T_\Gamma^{\text{II}}$ :** For the very definition of  $T_\Gamma^{\text{II}}$ , we have to specify the factorization prescription for the soft form factor  $\xi_\pi(E_2)$ . If we identify  $\xi_\pi(E_2)$  with the physical form factor  $f_+((p - k_2)^2)$  for  $B \rightarrow \pi$  vector transitions, with  $(p - k_2)^2 = M_B^2 - 2M_BE_2$ , we obtain

$$\phi_\pi(v) \frac{\phi_B^+(\omega)}{\omega} T_\Gamma^{\text{II}}(u, v, \omega, k^2, E_1, E_2) = g_{(A1-A6)}^{\text{finite}} + g_{(B1-B6)}^{\text{finite}} - g_+^{\text{finite}}(v, \omega, E_2) T_\Gamma^{\text{I}}(u, k^2, E_1, E_2). \quad (3.37)$$

Here the function  $g_{(A1-A6)}^{\text{finite}}$  and  $g_{(B1-B6)}^{\text{finite}}$  can be found in Eqs. (3.33), (3.34), (3.36), and the finite contributions to the  $B \rightarrow \pi$  form factor  $f_+(E_2)$  are encoded in the function  $g_+^{\text{finite}}$  as given in Eq. (B.4) in the appendix.



## 4 $B \rightarrow \pi\pi$ Form Factors and Observables

We are now going to briefly discuss some general phenomenological implications of the factorization formula (3.1) for the  $B \rightarrow \pi\pi$  form factors and  $B^- \rightarrow \pi^+\pi^-\ell^-\bar{\nu}_\ell$  decay observables in the kinematic region of small momentum transfer  $q^2$  and large dipion mass  $k^2$ .

### 4.1 Reduction of independent form factors in the QCDF limit

We first observe that the leading-twist contribution to the LO expression for the kernel  $T_\Gamma^{\text{I}}$  involves only two independent Dirac structures, see Eq. (3.13). Introducing

$$S_1(\Gamma) \equiv \left( \frac{2E_1 M_B}{k^2} - 1 \right) s_2 + \frac{1}{2} s_3, \quad S_2(\Gamma) \equiv s_1 + s_2 - \frac{M_B}{2E_2} s_5 - \frac{1}{2} s_7, \quad (4.1)$$

we thus have

$$\begin{aligned} & \langle \pi^+(k_1) \pi^-(k_2) | \bar{\psi}_u \Gamma \psi_b | B^-(p) \rangle \Big|_{\text{twist-2}} \\ & \simeq \frac{2\pi f_\pi}{k^2} \{ S_1(\Gamma) F_1(k^2, q^2, q \cdot \bar{k}) + S_2(\Gamma) F_2(k^2, q^2, q \cdot \bar{k}) \}, \end{aligned} \quad (4.2)$$

up to higher-order corrections in the strong coupling. The form factors  $F_{1,2}(k^2, q^2, q \cdot \bar{k})$  follow from the LO expression for the kernel  $T_\Gamma^{\text{I}}$  in (3.13),

$$F_{1,2}(k^2, q^2, q \cdot \bar{k}) \equiv \xi_\pi(E_2, \mu) \frac{i\alpha_s(\mu) C_F}{N_C} \int_0^1 du \phi_\pi(u, \mu) f_{1,2}(u), \quad (4.3)$$

where the functions  $f_{1,2}(u)$  are defined in Eq. (3.11), and the dependence on the kinematic variables follows from Eq. (2.5).

As explained above, the twist-3 contributions in (3.22) are formally power-suppressed, but numerically of the same order as the twist-2 terms because  $\mu_\pi/E_1 \simeq \mathcal{O}(1)$ , and therefore they have to be included as well. On the other hand, the spectator interactions contributing to the kernel  $T_\Gamma^{\text{II}}$  are suppressed by the strong coupling constant and can be neglected to first approximation.

#### 4.1.1 Relations among partial-wave form factors

	$S$ -wave	$P$ -wave	$D$ -wave
$F_0$	$\sqrt{\lambda}$	1	$\sqrt{\lambda}$
$F_t$	1	$\sqrt{\lambda}$	$\lambda$
$F_\perp$	—	$\sqrt{\lambda}$	$\lambda$
$F_\parallel$	—	1	$\sqrt{\lambda}$

**Table 2.** Scaling of partial-wave form factors as defined in Appendix A with  $\sqrt{\lambda}$ .

From (3.9) and (3.14) and (3.22) we can easily compute the leading contributions to vector and axial-vector form factors. To this end, we first project onto helicity form factors

as defined in [35] and summarized in Eq. (A.5) in the appendix. Using that for the phase space Scenarios A and B

$$q^2 \sim \sqrt{\lambda} \ll M_B^2,$$

each helicity form factor can then be expanded in the small parameter  $\Delta E_\pi/M_B \sim \sqrt{\lambda}/M_B^2$  which, via (2.4), translates into a power series in the angular variable  $z \equiv \cos \theta_\pi$ . From this, it is a straightforward task to identify the leading contributions to particular partial waves where – as a general rule, with one exception,<sup>4</sup> see Table 2 – higher partial waves will be suppressed by increasing powers of  $\sqrt{\lambda}/M_B$ . Performing the Gegenbauer expansion of the twist-2 pion LCDA to second order, the leading twist-2 and twist-3 contributions to the partial-wave form factors are obtained as

$$F_0^{(S)} \approx \frac{\sqrt{\lambda}}{2M_B\sqrt{q^2}} F_t^{(S)} \approx \frac{i\alpha_s C_F}{N_C} \frac{2\pi f_\pi}{M_B} \frac{2\sqrt{\lambda}}{M_B\sqrt{q^2}} \left(1 + \frac{3a_2^\pi}{4} + \frac{\mu_\pi}{M_B}\right) \xi_\pi\left(\frac{M_B}{2}\right), \quad (4.4)$$

and

$$F_0^{(P)} \simeq \frac{1}{\sqrt{2}} F_\parallel^{(P)} \approx \frac{2M_B\sqrt{q^2}}{\sqrt{\lambda}} F_t^{(P)} \approx -\frac{i\alpha_s C_F}{N_C} \frac{2\pi f_\pi}{M_B} \frac{2}{\sqrt{3}} \left(1 + \frac{3a_2^\pi}{2}\right) \xi_\pi\left(\frac{M_B}{2}\right), \quad (4.5)$$

and

$$\begin{aligned} F_0^{(D)} &\simeq \sqrt{\frac{2}{3}} F_\parallel^{(D)} \approx \frac{2M_B\sqrt{q^2}}{\sqrt{\lambda}} F_t^{(D)} \\ &\approx -\frac{i\alpha_s C_F}{N_C} \frac{2\pi f_\pi}{M_B} \frac{\sqrt{\lambda}}{6\sqrt{5}M_B^2} \left( (5 + 6a_2^\pi + \frac{2\mu_\pi}{M_B}) \xi_\pi\left(\frac{M_B}{2}\right) - (2 + 3a_2^\pi) M_B \xi'_\pi\left(\frac{M_B}{2}\right) \right), \end{aligned} \quad (4.6)$$

together with

$$F_\perp^{(P)} \approx \frac{i\alpha_s C_F}{N_C} \frac{2\pi f_\pi}{M_B} \frac{\sqrt{3}\sqrt{\lambda}}{\sqrt{2}M_B^2} \left(1 + a_2^\pi - \frac{\mu_\pi}{M_B}\right) \xi_\pi\left(\frac{M_B}{2}\right). \quad (4.7)$$

Notice that some of the above relations are a simple consequence of Lorentz invariance, as discussed in [41], since the number of independent 4-momentum vectors is reduced at the kinematic endpoint,  $\sqrt{\lambda} \rightarrow 0$ . In particular, we recover in that limit

$$F_0 \simeq \cos \theta_\pi F_\parallel \left(1 + \mathcal{O}\left(\frac{\sqrt{\lambda}}{M_B^2}\right)\right), \quad (4.8)$$

which implies  $F_\parallel^{(P)} \simeq \sqrt{2} F_0^{(P)}$ ,  $F_\parallel^{(D)} \simeq \frac{\sqrt{3}}{\sqrt{2}} F_0^{(D)}$  etc.

In order to assess the accuracy of the above relations, we study the form-factor ratios (properly normalized at  $q^2 \equiv 0$ ) as a function of the leptonic momentum transfer  $q^2$ .

---

<sup>4</sup>Notice that – in the considered kinematic region – the  $S$ -wave contribution to the form factor  $F_0$  is suppressed compared to the  $P$ -wave and of the same order as the  $D$ -wave. This differs from other kinematic situations as considered e.g. in [35]. In particular, the form factor  $F_0^{(D)}$  will now also provide a leading contribution to the forward-backward asymmetry with respect to the polar angle  $\theta_\pi$ .

parameter	value/interval	unit	prior	source/comments
QCD input parameter				
$\alpha_s(m_Z)$	$0.1184 \pm 0.0007$	—	gaussian @ 68%	[42]
$\mu$	$M_B/2 \pm M_B/4$	GeV	gaussian <sup>†</sup> @ 68%	
$\overline{m}_{u+d}(2 \text{ GeV})$	$7.8 \pm 0.9$	MeV	uniform @ 100%	see [43]
hadron masses				
$m_B$	5279.58	MeV	—	[42]
$m_\pi$	139.57	MeV	—	[42]
parameters of the pion DAs				
$f_\pi$	130.4	MeV	—	[42]
$a_2^\pi(1 \text{ GeV})$	[0.09, 0.25]	—	uniform @ 100%	[44]
$\mu_\pi(2 \text{ GeV})$	$2.5 \pm 0.3$	GeV	—	$m_\pi^2/(\overline{m}_{u+d})$

**Table 3.** The input parameters that were used in our numerical analysis. We express the prior distribution as a product of individual priors that are either uniform or gaussian. The uniform priors cover the stated intervals with 100% probability. The gaussian priors cover the stated intervals with 68% probability, and the central value corresponds to the mode of the prior. For practical purposes, variates from the gaussian priors are only drawn from their respective 99% probability intervals. The prior for the parameters describing the  $B \rightarrow \pi$  form factor  $f_+$  are not listed here, and taken from [43]. †: We artificially restrict the support of the renormalization scale  $\mu$  to the interval  $[M_B/4, M_B]$ .

The relations between the partial-wave projections for the form factors  $F_0$  and  $F_t$  receive corrections of order  $\sqrt{q^2}/M_B$  such that for  $q^2 \sim 0.3 \text{ GeV}^2$ , the deviations from (4.4 – 4.6) are expected to be of the order 10%. This is indeed the case for the  $S$ - and  $D$ -wave, while the corrections for the  $P$ -wave relation happen to imply large numerical pre-factors which can be traced back to the slope of the  $B \rightarrow \pi$  form factor at maximal recoil,  $\xi'_\pi(M_B/2)$ . On the other hand, the relations between the partial-wave projections for  $F_0$  and  $F_\parallel$  are protected by Lorentz symmetry (4.8), and only receive small corrections of order  $\sqrt{\lambda}/M_B^2$  which (in the kinematic situation we are considering) scales as  $q^2/M_B^2$ . These relations thus may still provide a reasonable approximation up to momentum transfers of order 1 GeV<sup>2</sup>.

## 4.2 Numerical results

In the following we will discuss numerical results for

- the partial-wave expansion of the form factors,
- and two observables in the differential decay width of  $B^- \rightarrow \pi^+ \pi^- \mu^- \bar{\nu}_\mu$ .

As already mentioned above, the corrections from spectator-scattering encoded in  $T_\Gamma^\Pi$  are a sub-leading effect and will be neglected for simplicity. Our prediction for the absolute

values of the form factors and decay width is still rather uncertain because of the overall factors of  $\alpha_s(\mu)$  and  $\xi_\pi(E_2, \mu)$ . As we will see, a reduction of the uncertainties induced by  $\xi_\pi$  and  $\alpha_s$  can be achieved through suitable arithmetic combinations of form factors or observables. For all numerical evaluations, we use the central values and uncertainty intervals for the input parameters as listed in Table 3, as well as the correlated results of [43] for the parameters describing the  $B \rightarrow \pi$  form factor  $f_+(\vec{q}^2)$  in the region  $0 \leq \vec{q}^2 \leq 12 \text{ GeV}^2$ . We find that the uncertainties due to the soft-form-factor parameters are in all cases smaller in size than the remaining parametric uncertainties, ranging from roughly 30%–90% of the non-form-factor uncertainties. (Note that we do not account for correlations between the  $B \rightarrow \pi$  form factor parameters and the parameters listed in Table 3.) The computations are made using the EOS software [45], which has been extended for this purpose.

**Partial-wave expansion.** We choose a benchmark point ( $q^2 = 0.6 \text{ GeV}^2, k^2 = 18.6 \text{ GeV}^2$ ), which corresponds to

$$\frac{q^2}{M_B^2} \approx 0.02, \quad \frac{\sqrt{\lambda}}{M_B^2} \approx 0.20,$$

in order to illustrate our results for the partial-wave expanded form factors. Each form factor is expanded up to its three leading partial waves, i.e. as a function of  $z \equiv \cos \theta_\pi$ , we have

$$F_{0(t)}^{S+P+D}(z) = F_{0(t)}^S + \sqrt{3} F_{0(t)}^P z + \sqrt{5} F_{0(t)}^D \frac{3z^2 - 1}{2}, \quad (4.9)$$

$$F_{\perp(\parallel)}^{P+D+F}(z) = \sqrt{\frac{3}{2}} F_{\perp(\parallel)}^P + \sqrt{\frac{15}{2}} F_{\perp(\parallel)}^D z + \sqrt{\frac{21}{4}} F_{\perp(\parallel)}^F \frac{5z^2 - 1}{2}, \quad (4.10)$$

where we have suppressed the  $q^2$  and  $k^2$  dependence of the form factors and partial-wave coefficients for brevity. One can now define relative residues

$$\begin{aligned} r_\lambda(z) &\equiv \frac{F_\lambda(z) - F_\lambda^{S+P+D}(z)}{F_\lambda(z)}, & \text{with } \lambda = 0, t, \\ r_\lambda(z) &\equiv \frac{F_\lambda(z) - F_\lambda^{P+D+F}(z)}{F_\lambda(z)}, & \text{with } \lambda = \perp, \parallel, \end{aligned} \quad (4.11)$$

in order to determine whether or not the form factors can be well approximated by their partial wave expansion. We find that

$$|r_0(z)| \leq 0.6\%, \quad |r_t(z)| \leq 3.0\%, \quad (4.12)$$

$$|r_\perp(z)| \leq 1.2\%, \quad |r_\parallel(z)| \leq 0.8\%. \quad (4.13)$$

We therefore conclude that the first three partial waves approximate the total  $\cos \theta_\pi$  dependence of the form factors well. These results are visualized in Fig. 3.

**Decay width and pionic forward-backward asymmetry.** Writing the 3-fold differential decay rate in terms of the kinematic variables ( $k^2, q^2, \cos \theta_\pi = \frac{2q \cdot \bar{k}}{\sqrt{\lambda}}$ ), we obtain in

phase space region	result			
	central	$\delta_{\text{param}}$	$\delta_{f_+}$	unit
$\mathcal{B}(B^- \rightarrow \pi^+ \pi^- \mu^- \bar{\nu}_\mu) /  V_{ub} ^2$				
(A)	2.93	+0.87 -0.40	+0.49 -0.35	$10^{-8}$
(B)	9.31	+2.70 -1.30	+1.77 -0.69	$10^{-7}$
(A+B)	9.60	+2.80 -1.30	+1.89 -0.79	$10^{-7}$
(C)	3.18	+0.63 -0.63	+0.48 -0.33	$10^{-5}$
$A_{\text{FB}}^\pi(B^- \rightarrow \pi^+ \pi^- \mu^- \bar{\nu}_\mu)$				
(A)	-1.96	+0.15 -0.19	+0.04 -0.07	$10^{-1}$
(B)	-0.29	+0.21 -0.19	+0.06 -0.11	$10^{-1}$
(A+B)	-0.32	+0.19 -0.21	+0.07 -0.11	$10^{-1}$
(C)	+1.25	+0.07 -0.07	+0.03 -0.08	$10^{-1}$

**Table 4.** Numerical estimates for the partially-integrated branching ratio (in units of  $|V_{ub}|^2$ ) and the pionic forward-backward asymmetry in different phase-space bins (see the text for more information). Note that our estimate for  $A_{\text{FB}}^\pi$  in the region (C) has been obtained for  $|\cos \theta_\pi| < 0.33$ . The variation of all parameters, except the  $B \rightarrow \pi$  form factor  $f_+$ , comprise the uncertainty denoted as  $\delta_{\text{param}}$ . The total uncertainty  $\delta_{\text{tot}}$  is then obtained as  $\delta_{\text{tot}}^2 = \delta_{\text{param}}^2 + \delta_{f_+}^2$ .

the SM (for unexpanded 2-pion form factors,  $F_i = F_i(k^2, q^2, q \cdot \bar{k})$ )<sup>5</sup>

$$\begin{aligned} & \frac{d^3 \Gamma(k^2, q^2, \cos \theta_\pi)}{dq^2 dk^2 d \cos \theta_\pi} \\ &= \frac{1}{4} |\mathcal{N}|^2 \beta_\ell \left[ (3 - \beta_\ell) |F_0|^2 + (1 - \cos^2 \theta_\pi) (3 - \beta_\ell) (|F_\parallel|^2 + |F_\perp|^2) + \frac{3m_\ell^2}{q^2} |F_t|^2 \right], \end{aligned} \quad (4.14)$$

where the normalization factor reads

$$|\mathcal{N}|^2 = G_F^2 |V_{ub}|^2 \frac{\beta_\ell q^2 \sqrt{\lambda}}{3 \cdot 2^{10} \pi^5 M_B^3}, \quad \text{with} \quad \beta_\ell = 1 - \frac{m_\ell^2}{q^2}. \quad (4.15)$$

The triple-differential branching ratio  $\mathcal{B}(k^2, q^2, \cos \theta_\pi)$  can be used to define the two observables that we wish to discuss: The partially-integrated branching ratio, as well as the pionic forward-backward asymmetry for the decay:

$$A_{\text{FB}}^\pi(k^2, q^2) \equiv \frac{\int_{-1}^{+1} d \cos \theta_\pi \text{sign}(\cos \theta_\pi) \mathcal{B}(k^2, q^2, \cos \theta_\pi)}{\int_{-1}^{+1} d \cos \theta_\pi \mathcal{B}(k^2, q^2, \cos \theta_\pi)}. \quad (4.16)$$

In order to avoid controversies with the choice of the input value for  $|V_{ub}|$ , we provide estimates for the branching ratio only in units of  $|V_{ub}|^2$ . Due to the smallness of the differential branching ratio, we prefer to provide our numerical estimates in form of binned

<sup>5</sup>Our result slightly disagrees with the  $\beta_\ell$  dependence in Eqs. (4.11) and (4.12) of [33] in the arXiv version v2.

observables. We consider the three phase-space bins following from our discussion in Sec. 2 for our numerical calculation (see also Fig. 4 for a visualization in the  $q^2$ – $k^2$  plane):

$$(A) : \begin{cases} 0.02 \text{ GeV}^2 \leq q^2 \leq (M_B - \sqrt{k^2})^2, \\ 18.60 \text{ GeV}^2 \leq k^2 \leq (M_B - \sqrt{q^2})^2, \\ -1 \leq \cos \theta_\pi \leq +1 \end{cases} \quad (4.17)$$

$$(B) : \begin{cases} 0.02 \text{ GeV}^2 \leq q^2 \leq (M_B - \sqrt{k^2})^2, \\ 13.90 \text{ GeV}^2 \leq k^2 \leq 18.60 \text{ GeV}^2, \\ -1 \leq \cos \theta_\pi \leq +1 \end{cases} \quad (4.18)$$

$$(C) : \begin{cases} 0.02 \text{ GeV}^2 \leq q^2 \leq (M_B - \sqrt{k^2})^2, \\ 7.00 \text{ GeV}^2 \leq k^2 \leq (M_B - \sqrt{q^2})^2, \\ -0.33 \leq \cos \theta_\pi \leq +0.33 \end{cases} \quad (4.19)$$

Region (A) corresponds to the phase space region in which the QCD-improved factorization results are expected to hold rigorously. Region (B) extrapolates to somewhat smaller values of  $k^2$  (and the quoted uncertainties for this region might be underestimated). Finally, region (C) limits the phase space for the helicity angle of the pions to  $|\cos \theta_\pi| \leq 0.33$ . This allows for using a larger part of the  $q^2$ – $k^2$  plane, while still enforcing large pion energies in the  $B$  rest frame,  $E_{1,2} > 1.24 \text{ GeV}$ . Our results for both observables are listed in Table 4. Moreover, we show the behaviour of the normalized single-differential decay rate as a function of  $\cos \theta_\pi$  in Fig. 5. As can be seen, the decay features a sizeable pionic forward-backward asymmetry in the phase-space bins (A) and (C). Note, that the asymmetry switches sign when enlarging the phase space toward bin (C). As a consequence, in the intermediate bin (B) the asymmetry is one order of magnitude smaller than in either (A) or (C).

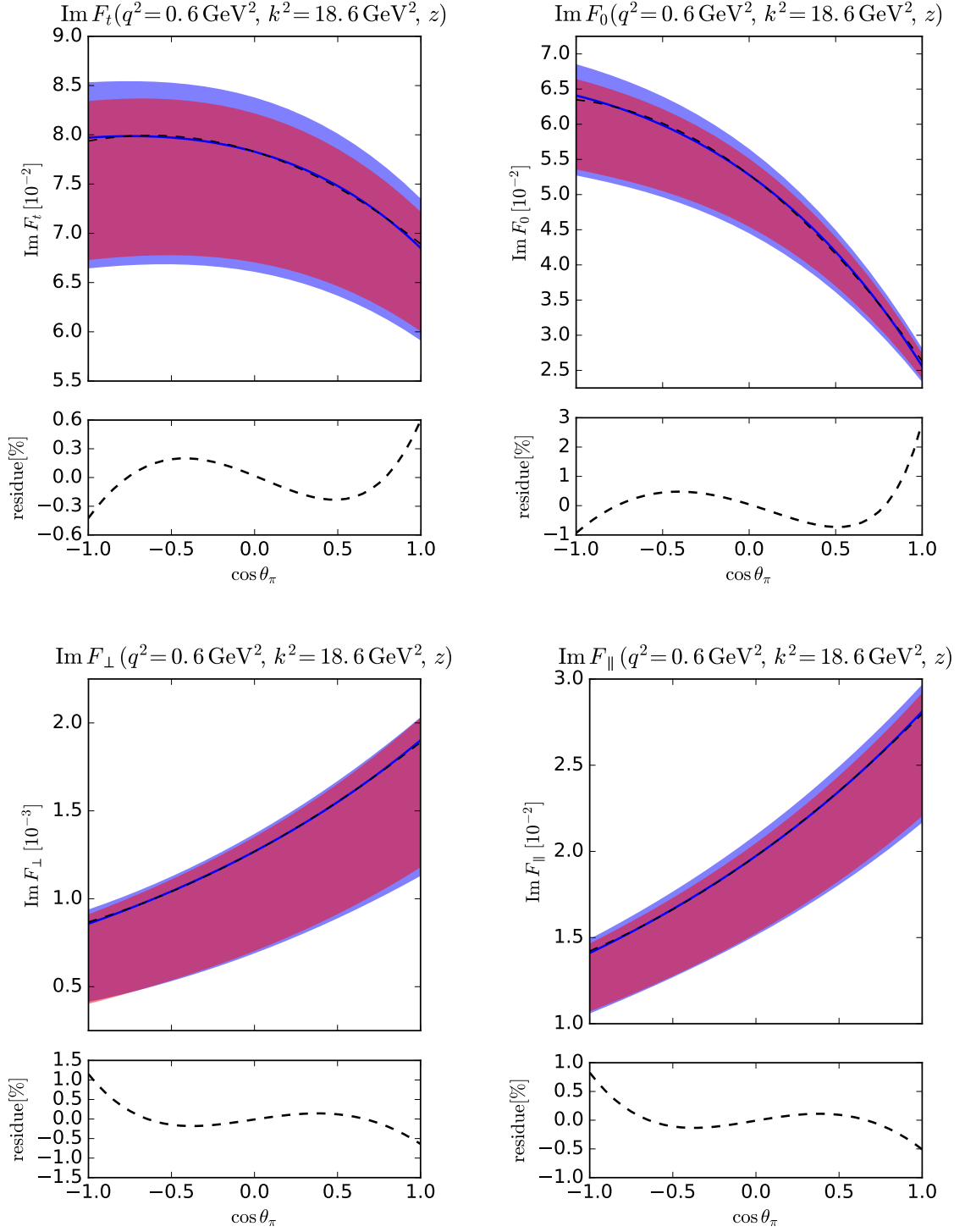


**Figure 3.** Plots of the  $\cos \theta_\pi$  dependence of the form factors in the phase space point  $(q^2 = 0.6 \text{ GeV}^2, k^2 = 18.6 \text{ GeV}^2)$ . The blue solid lines show the results at LO in  $\alpha_s$ , including both the twist-2 and twist-3 contributions. The blue shaded areas correspond to central 68% intervals of the posterior-predictive distributions, which arise from the variation of the input parameters as listed in Table 3 as well as the parameters for the  $B \rightarrow \pi$  form factor  $f_+$ . The red shaded area is the same as the blue area, except for the  $f_+$  variation. The black dashed lines show the approximation of each form factor by its first three partial waves. In the lower parts of each plot, the black dashed lines show the relative residue between the form factors and their partial-wave approximations. (Notice that in our convention, the form factors are purely imaginary at leading order.)

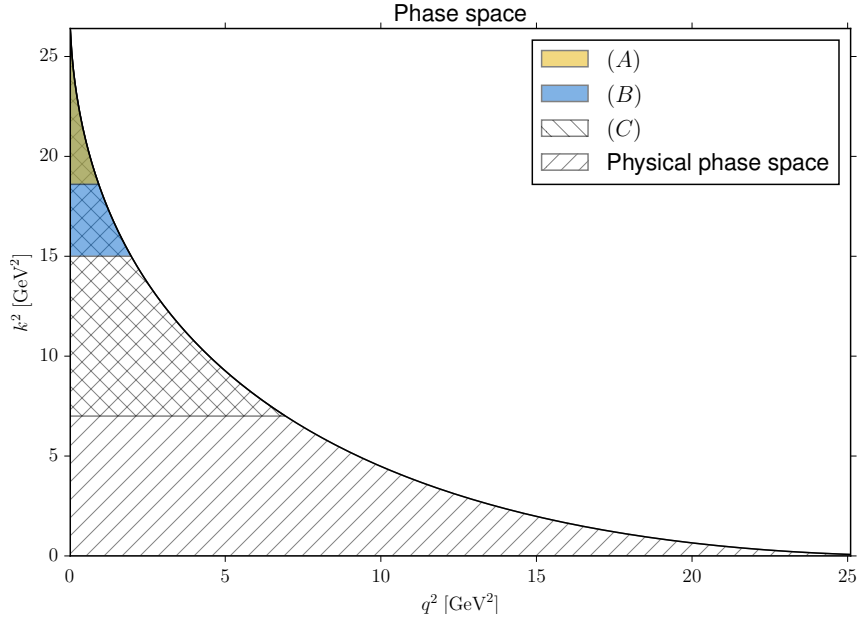


**Figure 4.** We show our choices of phase space bins for the QCDF region (A: gold) and the extrapolation (B: blue). The region C, which has additionally limitations on the magnitude of  $\cos \theta_\pi$ , is illustrated as the ‘\\’-hatched region. The remainder of the physical phase space is highlighted as the ‘//’-hatched area. Estimates for the integrated  $B^- \rightarrow \pi^+ \pi^- \mu^- \bar{\nu}_\mu$  observables in different bins are shown in Table 4.



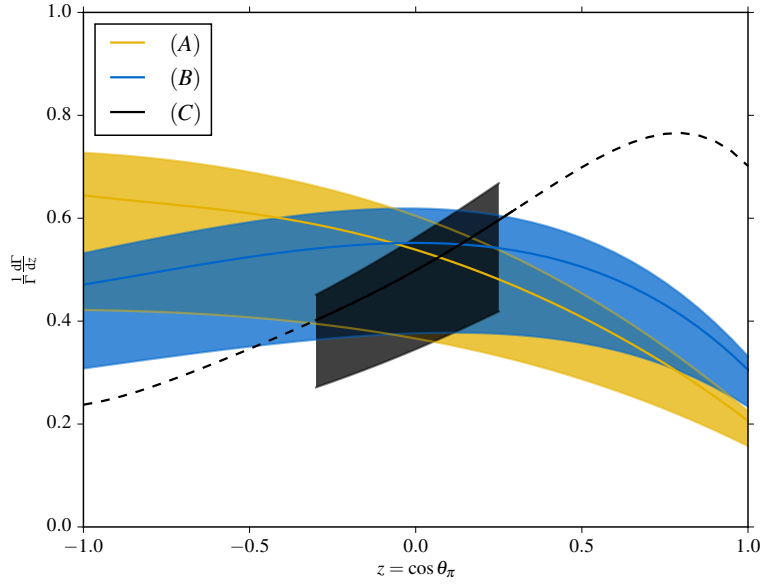


**Figure 5.** Plot of the single-differential normalized decay rate as a function of  $z \equiv \cos \theta_\pi$ . The gold and blue shaded areas correspond to the phase space bins (A) and (B) as defined in the text. The bin (C) has additional restrictions on the size of  $|z|$ . An extrapolation beyond these restrictions is indicated by the dashed curve. The shaded areas correspond to the 68% intervals as obtained from variation of all input parameters. The uncertainty is dominated by the parameters listed in Table 3.

## 5 Summary

In this work we have investigated the decay  $B^- \rightarrow \pi^+ \pi^- \ell^- \bar{\nu}_\ell$  in the context of QCD factorization (QCDF). To this end we have established a factorization formula for  $B \rightarrow \pi\pi$  form factors that is valid in the kinematic situation where both pions have large energy in the  $B$ -meson's rest frame with a large invariant dipion mass. The factorization formula takes a similar form as known from other applications of the QCDF approach, with one term depending on a universal “soft”  $B \rightarrow \pi$  form factor, and a second term which completely factorizes in terms of hadronic light-cone distribution amplitudes (LCDAs). The leading contributions to the corresponding short-distance kernels  $T^{\text{I}}$  and  $T^{\text{II}}$  have been calculated for arbitrary Dirac structures of the underlying  $b \rightarrow u$  transition current.

To first approximation, all dipion form factors are proportional to the strong coupling  $\alpha_s$  and the soft  $B \rightarrow \pi$  form factor, multiplied by linear combinations of only two independent convolution integrals involving the leading-twist LCDA of the positively charged pion. This results in approximate relations between the dipion form factors and their partial-wave components which have been worked out in detail. One class of corrections to the leading-order results arise from “chirally enhanced” power corrections to  $T^{\text{I}}$ . Neglecting 3-particle Fock states in the pion, the relevant twist-3 distribution amplitudes of the positively charged pion are completely fixed, and therefore no additional hadronic unknowns arise. The computation of the perturbative corrections due to spectator scattering, which is described by the short-distance kernel  $T^{\text{II}}$ , turns out to be more involved. The final result appears as a consequence of a delicate cancellation of endpoint-divergent terms between the individual diagrams and the corresponding terms in the soft  $B \rightarrow \pi$  form factor, providing a non-trivial confirmation of the factorization formula to the considered order in the perturbative expansion. The leading expression for  $T^{\text{II}}$  comes along with the first inverse moment of the  $B$ -meson LCDA. On the light meson's side, we find somewhat more complicated convolution integrals. In the large- $N_C$  limit they reduce to three independent functions that depend on the leading-twist pion LCDA.

In conclusion, the QCD factorization formula for  $B \rightarrow \pi\pi$  form factors at large dipion mass and its implications are interesting from both, the theoretical and phenomenological point of view. The factorization formula that we have established in this work combines features from semileptonic  $B \rightarrow \pi$  transitions and non-leptonic  $B \rightarrow \pi\pi$  decays with a non-trivial realization of the colour-transparency mechanism. Our results can also easily be generalized to other decay modes like  $B^- \rightarrow K^+ K^- \ell^- \bar{\nu}_\ell$  or  $\bar{B}_s \rightarrow \pi^+ K^0 \ell^- \bar{\nu}_\ell$ . Although the decay rate in the relevant kinematic region turns out to be too small to be of direct use for the determination of hadronic parameters or searches for new-physics effects, the approximate relations between the partial-wave form factors are useful for the phenomenological modelling of  $B \rightarrow \pi\pi\ell\nu$  decays over the whole physical phase space.

## Acknowledgements

We thank Bastian Müller for careful reading and checking of the manuscript. This work is supported in parts by the Bundesministerium für Bildung und Forschung (BMBF), and by the Deutsche Forschungsgemeinschaft (DFG) within Research Unit FOR 1873 (Quark Flavour Physics and Effective Field Theories). D.v.D. acknowledges support by the Swiss National Science Foundation under grant PP00P2-144674.

## A Definition of Dipion Form Factors

We follow the conventions in [35], and define vector and axial-vector form factors for  $b \rightarrow u$  currents in the SM as

$$\langle \pi^+(k_1) \pi^-(k_2) | \bar{\psi}_u \gamma^\mu \psi_b | B^-(p) \rangle = i F_\perp \frac{1}{\sqrt{k^2}} q_\perp^\mu, \quad (\text{A.1})$$

and

$$-\langle \pi^+(k_1) \pi^-(k_2) | \bar{\psi}_u \gamma^\mu \gamma_5 \psi_b | B^-(p) \rangle = F_t \frac{q^\mu}{\sqrt{q^2}} + F_0 \frac{2\sqrt{q^2}}{\sqrt{\lambda}} k_{(0)}^\mu + F_\parallel \frac{1}{\sqrt{k^2}} \bar{k}_\parallel^\mu, \quad (\text{A.2})$$

where

$$\begin{aligned} k_{(0)}^\mu &= k^\mu - \frac{k \cdot q}{q^2} q^\mu, \\ \bar{k}_\parallel^\mu &= \bar{k}^\mu - \frac{4(k \cdot q)(q \cdot \bar{k})}{\lambda} k^\mu + \frac{4k^2(q \cdot \bar{k})}{\lambda} q^\mu, \\ q_\perp^\mu &= 2 \epsilon^{\mu\alpha\beta\gamma} \frac{q_\alpha k_\beta \bar{k}_\gamma}{\sqrt{\lambda}}. \end{aligned} \quad (\text{A.3})$$

Here our convention for the Levi-Cevitá tensor is related to the definition of the Dirac matrix  $\gamma_5$  via

$$\text{tr} [\gamma_5 \gamma^\mu \gamma^\nu \gamma^\rho \gamma^\sigma] = -4i \epsilon^{\mu\nu\rho\sigma}. \quad (\text{A.4})$$

In terms of the so-defined “helicity form factors”, one obtains simple expressions for the differential decay width and the angular observables, and simple relations between form factors in HQET or SCET, which has also been emphasized for other decay modes [31, 46–49]. To extract the individual form factors, the above relations can be simply inverted,

$$\begin{aligned} F_\perp(k^2, q^2, q \cdot \bar{k}) &= -\frac{i\sqrt{k^2}}{q_\perp^2} \langle \pi^+ \pi^- | \bar{\psi}_u \not{q}_\perp \psi_b | B^- \rangle, \\ F_\parallel(k^2, q^2, q \cdot \bar{k}) &= -\frac{\sqrt{k^2}}{\bar{k}_\parallel^2} \langle \pi^+ \pi^- | \bar{\psi}_u \not{\bar{k}}_\parallel \gamma_5 \psi_b | B^- \rangle, \\ F_0(k^2, q^2, q \cdot \bar{k}) &= -\frac{\sqrt{\lambda}}{2\sqrt{q^2} k_{(0)}^2} \langle \pi^+ \pi^- | \bar{\psi}_u \not{k}_{(0)} \gamma_5 \psi_b | B^- \rangle, \\ F_t(k^2, q^2, q \cdot \bar{k}) &= -\frac{1}{\sqrt{q^2}} \langle \pi^+ \pi^- | \bar{\psi}_u \not{q} \gamma_5 \psi_b | B^- \rangle, \end{aligned} \quad (\text{A.5})$$

where

$$q_{\perp}^2 = \bar{k}_{\parallel}^2 = -\frac{k^2 (4E_1 E_2 - k^2)}{(E_1 + E_2)^2 - k^2}, \quad k_{(0)}^2 = -\frac{M_B^2 ((E_1 + E_2)^2 - k^2)}{q^2}. \quad (\text{A.6})$$

These form factors can be further expanded in terms of partial waves (see e.g. [35]), using

$$\begin{aligned} F_{\perp,\parallel}^{(\ell)} &= -\int_{-1}^{+1} dz \frac{\sqrt{2\ell+1}}{2} F_{\perp,\parallel}(z) p_{\ell}^1(z) \sqrt{1-z^2}, \\ F_{0,t}^{(\ell)} &= +\int_{-1}^{+1} dz \frac{\sqrt{2\ell+1}}{2} F_{0,t}(z) p_{\ell}^0(z), \end{aligned} \quad (\text{A.7})$$

where  $p_{\ell}^m(z)$  denote the *symmetrised* associated Legendre polynomials,

$$p_{\ell}^m(z) \equiv \sqrt{\frac{(\ell-m)!}{(\ell+m)!}} P_{\ell}^m(z), \quad (\text{A.8})$$

which fulfill the orthogonality relations

$$\int_{-1}^{+1} dz p_{\ell}^m(z) p_k^m(z) = \frac{2}{2\ell+1} \delta_{\ell k}, \quad (\text{A.9})$$

and  $z \equiv \cos \theta_{\pi} = \frac{2q \cdot \bar{k}}{\sqrt{\lambda}}$ . Notice that in our convention the form factors turn out to be purely imaginary at leading order.

## B Detailed Calculation for Kernel $T^{\text{II}}$

In the following we summarize the individual results for the spectator-scattering diagrams that contribute to the kernel  $T^{\text{II}}$  at LO. We find it convenient to split the expressions into two terms: one representing the individual contributions to the subprocess  $b \rightarrow d\pi^+ g\ell^- \bar{\nu}_{\ell}$ , and the other the hard-collinear interaction with the spectator quark which induces the  $B^- \rightarrow \pi^-$  transition, such that generically we have

$$\langle \pi\pi | \bar{\psi}_u \Gamma \psi_b | B \rangle \Big|_{\text{Diagram X}} = \text{tr} [A_X A^{\text{spec}}], \quad (\text{B.1})$$

with

$$A^{\text{spec}} = -g_s T^B \frac{\mathcal{M}_{B\gamma\beta} \mathcal{M}_{\pi^-}}{(\ell - k_{\bar{q}2})^2} \simeq g_s T^B \frac{\mathcal{M}_{B\gamma\beta} \mathcal{M}_{\pi^-}}{2\bar{\nu}\omega E_2}. \quad (\text{B.2})$$

Here the trace runs over Dirac and colour indices, and the integration over the (light-cone) momenta of the quarks is understood implicitly. The factor  $(-i)$  from the hard-collinear gluon propagator (in Feynman gauge) and the minus sign from the trace over the closed fermion loop has been assigned to the spectator term. If we restrict ourselves to the leading-power contributions in the  $1/m_b$  expansion, we can neglect the external transverse momenta in the *hard* sub-process. However, as is known and understood from the analogous case of  $B \rightarrow \pi\ell\nu$  transitions [24, 27, 28], the impact of transverse momenta in the hard-collinear spectator scattering is more subtle, and as a consequence transverse momenta in the associated propagator numerators must not be neglected from the very beginning. The resulting contribution to the  $B \rightarrow \pi\pi$  matrix element will be decomposed according to (3.26).

### B.1 Recapitulation: the $B \rightarrow \pi$ form factor $f_+$

In this paper, we will use a physical definition of the soft  $B \rightarrow \pi$  form factor  $\xi_\pi(E_2)$ . To this end, we will identify it with the physical form factor  $f_+((p-k_2)^2)$ , where  $(p-k_2)^2 = M_B^2 - 2M_B E_2$ . The leading-power spectator-scattering contributions to  $f_+$  have been calculated in [24] and amount to

$$\begin{aligned} \xi_\pi^{(\text{HSA})}(E_2) &\equiv f_+^{(\text{HSA})}(E_2) \\ &= \frac{\alpha_s}{4\pi} \frac{\pi^2 f_B f_\pi M_B}{N_C E_2^2} \int_0^1 dv \int_0^\infty d\omega \left( g_+^{\text{finite}}(v, \omega, E_2) + g_+^{\text{endpoint}}(v, \omega, E_2) \right), \end{aligned} \quad (\text{B.3})$$

with

$$g_+^{\text{finite}}(v, \omega, E_2) = C_F \frac{4E_2 - M_B}{M_B} \frac{\phi_\pi(v)}{\bar{v}} \frac{\phi_B^+(\omega)}{\omega}, \quad (\text{B.4})$$

and

$$\begin{aligned} g_+^{\text{endpoint}}(v, \omega, E_2) &= C_F \frac{(1+\bar{v}) \phi_\pi(v)}{\bar{v}^2} \frac{\phi_B^-(\omega)}{\omega} + 2\mu_\pi \frac{\phi_P(v)}{\bar{v}} \frac{\phi_B^+(\omega)}{\omega^2} \\ &\quad + \frac{\mu_\pi}{2E_2} \left( \frac{\phi_P(v) - \phi'_\sigma(v)/6}{\bar{v}^2} \right) \frac{\phi_B^+(\omega)}{\omega}. \end{aligned} \quad (\text{B.5})$$

Here the scaling of the various moments (after some ad-hoc regularization,  $\bar{v} \gtrsim \frac{\Lambda}{M_B}$ ,  $\omega \gtrsim \frac{\Lambda^2}{M_B}$ ) is to be understood as [24]

$$\begin{aligned} \left\langle \frac{\phi_\pi(v)}{\bar{v}} \right\rangle &\sim \mathcal{O}(1), \\ \left\langle \frac{\phi_P(v) + \phi'_\sigma(v)/6}{\bar{v}^2} \right\rangle &\sim \left\langle \frac{\phi_P(v)}{\bar{v}} \right\rangle \sim \left\langle \frac{\phi_\pi(v)}{\bar{v}^2} \right\rangle \sim \mathcal{O}\left(\ln \frac{\Lambda}{M_B}\right), \\ \left\langle \frac{\phi_P(v) - \phi'_\sigma(v)/6}{\bar{v}^2} \right\rangle &\sim \left\langle \frac{\phi_P(v)}{\bar{v}^2} \right\rangle \sim \mathcal{O}\left(\frac{M_B}{\Lambda}\right), \end{aligned} \quad (\text{B.6})$$

and

$$\left\langle \frac{\phi_B^+(\omega)}{\omega} \right\rangle = \mathcal{O}\left(\frac{1}{\Lambda}\right), \quad \left\langle \frac{\phi_B^+(\omega)}{\omega^2} \right\rangle \sim \mathcal{O}\left(\frac{1}{\Lambda^2} \ln \frac{\Lambda}{M_B}\right), \quad \left\langle \frac{\phi_B^-(\omega)}{\omega} \right\rangle = \mathcal{O}\left(\frac{1}{\Lambda} \ln \frac{\Lambda}{M_B}\right). \quad (\text{B.7})$$

In the following we have to show that the structures in  $g_+^{\text{endpoint}}$  are indeed universal, and also appear in exactly the same form in the spectator-scattering contributions to the  $B \rightarrow \pi\pi$  form factors at large  $k^2$ , justifying the procedure employed around (3.9).

### B.2 Expressions for $b \rightarrow d\pi^+ g\ell^- \bar{\nu}_\ell$ amplitudes

In the following, we collect the amplitudes  $A_X$  describing the  $b \rightarrow d\pi^+ g\ell^- \bar{\nu}_\ell$  subprocess in (B.1) from the various diagrams, together with the approximations to be made in the large-recoil limit.

### B.2.1 Diagrams (A1-A6)

$$\begin{aligned}
A_1 &= 4\pi\alpha_s C_F g_s T^B \frac{\gamma^\alpha \mathcal{M}_{\pi^+}^{(2)} \gamma_\alpha (\not{k}_1 + \not{k}_{q2}) \Gamma (\not{p} - \not{k}_{\bar{q}2} + m_b) \gamma^\beta}{(k_1 + k_{q2})^2 (k_{q2} + k_{\bar{q}1})^2 ((p_b - k_{\bar{q}2})^2 - m_b^2)} \\
&\simeq -4\pi\alpha_s C_F g_s T^B \frac{\mathcal{M}_{\pi^+}^{(2)} \not{k}_2 \Gamma (\not{p} + M_B - \bar{v} \not{k}_2) \gamma^\beta}{\bar{u} v \bar{v} M_B E_2 (k^2)^2}, \tag{B.8}
\end{aligned}$$

$$\begin{aligned}
A_2 &= 4\pi\alpha_s C_F g_s T^B \frac{\gamma^\beta (\not{k}_2 - \not{\ell}) \gamma^\alpha \mathcal{M}_{\pi^+}^{(2)} \gamma_\alpha (\not{k} - \not{\ell}) \Gamma}{(k_2 - \ell)^2 (k - \ell)^2 (k - \ell - k_{q1})^2} \\
&\simeq -4\pi\alpha_s C_F g_s T^B \frac{\gamma^\beta (\not{k}_2 - \not{\ell}) \mathcal{M}_{\pi^+}^{(2)} \not{k}_2 \Gamma}{\bar{u} \omega E_2 (k^2)^2}, \tag{B.9}
\end{aligned}$$

and

$$\begin{aligned}
A_3 &= -4\pi\alpha_s C_{FA} g_s T^B \frac{\gamma^\alpha \mathcal{M}_{\pi^+}^{(2)} \gamma^\beta (\not{k}_{q1} + \not{k}_{\bar{q}2} - \not{\ell}) \gamma_\alpha (\not{k} - \not{\ell}) \Gamma}{(k_{q1} + k_{\bar{q}2} - \ell)^2 ((k - \ell)^2 (k_{q1} + k_{q2})^2)} \\
&\simeq -4\pi\alpha_s C_{FA} g_s T^B \frac{\gamma^\alpha \mathcal{M}_{\pi^+}^{(2)} \gamma^\beta (u \not{k}_1 + \bar{v} \not{k}_2) \gamma_\alpha \not{k} \Gamma}{u \bar{u} v \bar{v} (k^2)^3}, \tag{B.10}
\end{aligned}$$

$$\begin{aligned}
A_4 &= -4\pi\alpha_s C_{FA} g_s T^B \frac{\gamma^\alpha (\not{l} - \not{k}_{\bar{q}1} - \not{k}_{\bar{q}2}) \gamma^\beta \mathcal{M}_{\pi^+}^{(2)} \gamma_\alpha (\not{k} - \not{\ell}) \Gamma}{(\ell - k_{\bar{q}1} - k_{\bar{q}2})^2 ((k - \ell)^2 (k_{q1} + k_2 - \ell)^2)} \\
&\simeq 4\pi\alpha_s C_{FA} g_s T^B \frac{\gamma^\alpha (\bar{u} \not{k}_1 + \bar{v} \not{k}_2) \gamma^\beta \mathcal{M}_{\pi^+}^{(2)} \gamma_\alpha \not{k} \Gamma}{\bar{u}^2 \bar{v} (k^2)^3}, \tag{B.11}
\end{aligned}$$

and

$$\begin{aligned}
A_5 &= 4\pi\alpha_s C_F g_s T^B \frac{\gamma^\alpha \mathcal{M}_{\pi^+}^{(2)} \gamma_\alpha (\not{k}_1 + \not{k}_{q2}) \gamma^\beta (\not{k} - \not{\ell}) \Gamma}{(k_1 + k_{q2})^2 ((k - \ell)^2 (k_{\bar{q}1} + k_{q2})^2)} \\
&\simeq 8\pi\alpha_s C_F g_s T^B \frac{\mathcal{M}_{\pi^+}^{(2)} \not{k}_2 \gamma^\beta \not{k} \Gamma}{\bar{u} v (k^2)^3}, \tag{B.12}
\end{aligned}$$

and

$$\begin{aligned}
A_6 &= 4\pi\alpha_s \frac{C_A}{2} g_s T^B \frac{\gamma_\alpha \mathcal{M}_{\pi^+}^{(2)} \gamma_\gamma (\not{k} - \not{\ell}) \Gamma}{(k - \ell)^2 (k_{\bar{q}1} + k_2 - \ell)^2 (k_{\bar{q}1} + k_{q2})^2} \\
&\quad \times \left( g^{\alpha\beta} (k_{\bar{q}2} - k_{q2} - k_{\bar{q}1} - \ell)^\gamma + g^{\beta\gamma} (2\ell - k_{\bar{q}1} - k_2 - k_{\bar{q}2})^\alpha \right. \\
&\quad \left. + g^{\alpha\gamma} (2k_{\bar{q}1} + k_2 + k_{q2} - \ell)^\beta \right) \\
&\simeq 2\pi\alpha_s C_A g_s T^B \frac{\gamma_\alpha \mathcal{M}_{\pi^+}^{(2)} \gamma_\gamma \not{k} \Gamma}{\bar{u}^2 v (k^2)^3} \\
&\quad \times \left( g^{\alpha\beta} (\bar{v} - v) k_2^\gamma - g^{\beta\gamma} (1 + \bar{v}) k_2^\alpha + g^{\alpha\gamma} (2\bar{u} k_1 + (1 + v) k_2)^\beta \right). \tag{B.13}
\end{aligned}$$

### B.2.2 Diagrams (B1-B6)

$$\begin{aligned}
B_1 &= 4\pi\alpha_s C_F g_s T^B \frac{\gamma^\alpha \mathcal{M}_{\pi^+}^{(2)} \Gamma(\not{p} - \not{k}_{\bar{q}1} - \not{k}_2 + m_b) \gamma_\alpha (\not{p} - \not{k}_{\bar{q}2} + m_b) \gamma^\beta}{((p - k_{\bar{q}1} - k_2)^2 - m_b^2) ((p - k_{\bar{q}2})^2 - m_b^2) (k_{\bar{q}1} + k_{q2})^2} \\
&\simeq -4\pi\alpha_s C_F g_s T^B \frac{\gamma^\alpha \mathcal{M}_{\pi^+}^{(2)} \Gamma(\not{p} - \bar{u}\not{k}_1 - \not{k}_2 + M_B) \gamma_\alpha (\not{p} - \bar{v}\not{k}_2 + M_B) \gamma^\beta}{2\bar{u}\bar{v} E_2 M_B k^2 (-2\bar{u}E_1 M_B - 2E_2 M_B + \bar{u}k^2)},
\end{aligned} \tag{B.14}$$

$$\begin{aligned}
B_2 &= 4\pi\alpha_s C_F g_s T^B \frac{\gamma^\beta (\not{k}_2 - \not{\ell}) \gamma^\alpha \mathcal{M}_{\pi^+}^{(2)} \Gamma(\not{p} - \not{k}_{\bar{q}1} - \not{k}_2 - \not{\ell} + m_b) \gamma_\alpha}{(k_2 - \ell)^2 ((p - k_{\bar{q}1} - k_2 - \ell)^2 - m_b^2) (k_{\bar{q}1} + k_2 - \ell)^2} \\
&\simeq -4\pi\alpha_s C_F g_s T^B \frac{\gamma^\beta (\not{k}_2 - \not{\ell}) \gamma^\alpha \mathcal{M}_{\pi^+}^{(2)} \Gamma(\not{p} - \bar{u}\not{k}_1 - \not{k}_2 + M_B) \gamma_\alpha}{2\bar{u} \omega E_2 k^2 (-2\bar{u}E_1 M_B - 2E_2 M_B + \bar{u}k^2)},
\end{aligned} \tag{B.15}$$

and

$$\begin{aligned}
B_3 &= -4\pi\alpha_s C_{FA} g_s T^B \frac{\gamma^\alpha \mathcal{M}_{\pi^+}^{(2)} \gamma^\beta (\not{k}_{q1} + \not{k}_{\bar{q}2} - \not{\ell}) \Gamma(\not{p} - \not{k}_{\bar{q}1} - \not{k}_{q2} - \not{\ell} + m_b) \gamma_\alpha}{(k_{q1} + k_{\bar{q}2} - \ell)^2 ((p - k_{\bar{q}1} - k_{q2} - \ell)^2 - m_b^2) (k_{\bar{q}1} + k_{q2})^2} \\
&\simeq -4\pi\alpha_s C_{FA} g_s T^B \frac{\gamma^\alpha \mathcal{M}_{\pi^+}^{(2)} \gamma^\beta (u\not{k}_1 + \bar{v}\not{k}_2) \Gamma(\not{p} - \bar{u}\not{k}_1 - v\not{k}_2 + M_B) \gamma_\alpha}{u\bar{u} v\bar{v} (k^2)^2 (-2\bar{u}E_1 M_B - 2vE_2 M_B + \bar{u}vk^2)},
\end{aligned} \tag{B.16}$$

$$\begin{aligned}
B_4 &= -4\pi\alpha_s C_{FA} g_s T^B \frac{\gamma^\alpha (-\not{k}_{\bar{q}1} - \not{k}_{\bar{q}2} + \not{\ell}) \gamma^\beta \mathcal{M}_{\pi^+}^{(2)} \Gamma(\not{p} - \not{k}_{\bar{q}1} - \not{k}_2 + m_b) \gamma_\alpha}{(k_{\bar{q}1} + k_{\bar{q}2} - \ell)^2 ((p - k_{\bar{q}1} - k_2)^2 - m_b^2) (k_{\bar{q}1} + k_2 - \ell)^2} \\
&\simeq -4\pi\alpha_s C_{FA} g_s T^B \frac{\gamma^\alpha (-\bar{u}\not{k}_1 - \bar{v}\not{k}_2) \gamma^\beta \mathcal{M}_{\pi^+}^{(2)} \Gamma(\not{p} - \bar{u}\not{k}_1 - \not{k}_2 + M_B) \gamma_\alpha}{\bar{u}^2 \bar{v} (k^2)^2 (-2\bar{u}E_1 M_B - 2E_2 M_B + \bar{u}k^2)},
\end{aligned} \tag{B.17}$$

$$\begin{aligned}
B_5 &= -4\pi\alpha_s C_{FA} g_s T^B \frac{\gamma^\alpha \mathcal{M}_{\pi^+}^{(2)} \Gamma(\not{p} - \not{k}_{\bar{q}1} - \not{k}_2 + m_b) \gamma^\beta (\not{p} - \not{k}_{\bar{q}1} - \not{k}_{q2} - \not{\ell} + m_b) \gamma_\alpha}{((p - k_{\bar{q}1} - k_2)^2 - m_b^2) ((p - k_{\bar{q}1} - k_{q2} - \ell)^2 - m_b^2) (k_{\bar{q}1} + k_{q2})^2} \\
&\simeq -4\pi\alpha_s C_{FA} g_s T^B \\
&\quad \times \frac{\gamma^\alpha \mathcal{M}_{\pi^+}^{(2)} \Gamma(\not{p} - \bar{u}\not{k}_1 - \not{k}_2 + M_B) \gamma^\beta (\not{p} - \bar{u}\not{k}_1 - v\not{k}_2 + M_B) \gamma_\alpha}{(-2\bar{u}M_B E_1 - 2M_B E_2 + \bar{u}k^2) (-2\bar{u}M_B E_1 - 2vM_B E_2 + \bar{u}vk^2) \bar{u}vk^2},
\end{aligned} \tag{B.18}$$

and

$$\begin{aligned}
B_6 &= 4\pi\alpha_s \frac{C_A}{2} g_s T^B \frac{\gamma_\alpha \mathcal{M}_{\pi^+}^{(2)} \Gamma(\not{p} - \not{k}_{\bar{q}1} - \not{k}_2 + m_b) \gamma_\gamma}{((p - k_{\bar{q}1} - k_2)^2 - m_b^2) (k_{\bar{q}1} + k_2 - \ell)^2 (k_{\bar{q}1} + k_{q2})^2} \\
&\quad \times \left( g^{\alpha\beta} (k_{\bar{q}2} - k_{q2} - k_{\bar{q}1} - \ell)^\gamma + g^{\beta\gamma} (2\ell - k_{\bar{q}1} - k_2 - k_{\bar{q}2})^\alpha \right. \\
&\quad \left. + g^{\alpha\gamma} (2k_{\bar{q}1} + k_2 + k_{q2} - \ell)^\beta \right) \\
&\simeq 2\pi\alpha_s C_A g_s T^B \frac{\gamma_\alpha \mathcal{M}_{\pi^+}^{(2)} \Gamma(\not{p} - \bar{u}\not{k}_1 - \not{k}_2 + M_B) \gamma_\gamma}{(-2\bar{u}E_1 M_B - 2E_2 M_B + \bar{u}k^2) \bar{u}^2 v (k^2)^2} \\
&\quad \times \left( g^{\alpha\beta} ((\bar{v} - v) k_2 - \bar{u}k_1)^\gamma - g^{\beta\gamma} (1 + \bar{v}) k_2^\alpha + g^{\alpha\gamma} (2\bar{u}k_1 + vk_2)^\beta \right).
\end{aligned} \tag{B.19}$$

### B.3 Contributions to $B \rightarrow \pi\pi$ matrix elements

In the following we collect the finite and endpoint divergent contributions of the individual Feynman diagrams to the  $B \rightarrow \pi\pi$  matrix elements as defined in Eq. (3.26). The contributions to the kernel  $T_{\Gamma}^{\text{II}}$  from the spectator scattering diagrams are expressed in terms of several functions of the momentum fractions  $\bar{u}$  and  $\bar{v}$  of the (anti-)quarks in the two pions which are convoluted with the corresponding leading-twist LCDAs. In the following we use the same abbreviations for Dirac traces (3.10), kinematic invariants (3.27), colour factors (3.28) as defined in the main body of the article. We also employ the equations of motion (3.29) to simplify the twist-3 contributions to the endpoint-divergent terms in the hard-scattering amplitudes.

#### B.3.1 Diagram (A1)

$$g_{(A1)}^{\text{finite}} = C_F \frac{E_2}{M_B} \frac{s_4}{\bar{u}} \frac{\phi_{\pi}(v)}{v\bar{v}} \frac{\phi_B^+(\omega)}{\omega} \quad (\text{B.20})$$

and

$$g_{(A1)}^{\text{endpoint}} = C_F \frac{S_A}{\bar{u}} \left( \frac{\phi_{\pi}(v)}{v\bar{v}^2} \frac{\phi_B^-(\omega)}{\omega} + \frac{\mu_{\pi}\phi_{\sigma}(v)}{6E_2\bar{v}^3} \frac{\phi_B^+(\omega)}{\omega} \right) \quad (\text{B.21})$$

#### B.3.2 Diagram (A2)

$$g_{(A2)}^{\text{finite}} = C_F \left( \frac{2E_2M_B}{k^2} \frac{s_6}{\bar{u}} - \frac{s_2}{\bar{u}} \right) \frac{\phi_{\pi}(v)}{\bar{v}} \frac{\phi_B^+(\omega)}{\omega}, \quad (\text{B.22})$$

and

$$g_{(A2)}^{\text{endpoint}} = C_F \frac{S_A}{\bar{u}} \left( \frac{\phi_{\pi}(v)}{\bar{v}} \frac{\phi_B^-(\omega)}{\omega} + 2\mu_{\pi} \frac{\phi_P(v)}{\bar{v}} \frac{\phi_B^+(\omega)}{\omega^2} \right). \quad (\text{B.23})$$

#### B.3.3 Diagrams (A3+A4)

$$g_{(A3+A4)}^{\text{finite}} = C_{FA} \left( \frac{2E_2M_B}{k^2} \frac{s_6}{\bar{u}} - \frac{s_2}{\bar{u}} \right) \frac{\phi_{\pi}(v)}{v\bar{v}} \frac{\phi_B^+(\omega)}{\omega}, \quad (\text{B.24})$$

and

$$g_{(A3+A4)}^{\text{endpoint}} = -C_{FA} \left( \frac{2E_2M_B}{k^2} \frac{s_5}{\bar{u}^2} \frac{\phi_{\pi}(v)}{\bar{v}} \frac{\phi_B^+(\omega)}{\omega} - \frac{S_A}{\bar{u}} \frac{\phi_{\pi}(v)}{v\bar{v}} \frac{\phi_B^-(\omega)}{\omega} \right). \quad (\text{B.25})$$



#### B.3.4 Diagram (A5)

$$g_{(A5)}^{\text{finite}} = C_F \frac{2E_2 M_B}{k^2} \frac{s_5}{\bar{u}} \frac{\phi_\pi(v)}{v\bar{v}} \frac{\phi_B^+(\omega)}{\omega}, \quad (\text{B.26})$$

and

$$g_{(A5)}^{\text{endpoint}} = 0. \quad (\text{B.27})$$

#### B.3.5 Diagram (A6)

$$g_{(A6)}^{\text{finite}} = C_A \left( \frac{s_2}{\bar{u}} - \frac{2E_2 M_B}{k^2} \frac{s_6}{\bar{u}} \right) \frac{\phi_\pi(v)}{2v\bar{v}} \frac{\phi_B^+(\omega)}{\omega}, \quad (\text{B.28})$$

and

$$g_{(A6)}^{\text{endpoint}} = C_A \left( \frac{2E_2 M_B}{k^2} \frac{s_5}{\bar{u}^2} \frac{(v - \bar{v}) \phi_\pi(v)}{4v\bar{v}} \frac{\phi_B^+(\omega)}{\omega} - \frac{S_A}{\bar{u}} \frac{\phi_\pi(v)}{2v\bar{v}} \frac{\phi_B^-(\omega)}{\omega} \right). \quad (\text{B.29})$$

#### B.3.6 Diagram (B1)

$$g_{(B1)}^{\text{finite}} = C_F \frac{2E_2}{M_B} \frac{S_B^{(i)}(u)}{\bar{u}} \frac{\phi_\pi(v)}{v\bar{v}} \frac{\phi_B^+(\omega)}{\omega}, \quad (\text{B.30})$$

and

$$g_{(B1)}^{\text{endpoint}} = C_F \frac{S_B^{(i)}(u) + S_B^{(ii)}(u)}{\bar{u}} \left( \frac{\phi_\pi(v)}{v\bar{v}^2} \frac{\phi_B^-(\omega)}{\omega} + \frac{\mu_\pi \phi_\sigma(v)}{6E_2 \bar{v}^3} \frac{\phi_B^+(\omega)}{\omega} \right). \quad (\text{B.31})$$

#### B.3.7 Diagram (B2)

$$g_{(B2)}^{\text{finite}} = C_F \left( \left( \frac{2E_2}{M_B} - 1 \right) \frac{S_B^{(i)}(u)}{\bar{u}} + \frac{E_2}{M_B} \frac{s_3}{\bar{u}} \right) \frac{\phi_\pi(v)}{\bar{v}} \frac{\phi_B^+(\omega)}{\omega}, \quad (\text{B.32})$$

and

$$g_{(B2)}^{\text{endpoint}} = C_F \frac{S_B^{(i)}(u) + S_B^{(ii)}(u)}{\bar{u}} \left( \frac{\phi_\pi(v)}{\bar{v}} \frac{\phi_B^-(\omega)}{\omega} + 2\mu_\pi \frac{\phi_P(v)}{\bar{v}} \frac{\phi_B^+(\omega)}{\omega^2} \right). \quad (\text{B.33})$$

### B.3.8 Diagrams (B3+B5)

$$g_{(B3+B5)}^{\text{finite}} = C_{FA} \left( -v_{\perp}^2 \frac{S_B^{(i)}(u)}{\bar{u}} \left( 1 - \frac{2E_2 M_B}{\bar{u} v k^2 - 2\bar{u} E_1 M_B - 2v E_2 M_B} \right) + \frac{2E_2^2 s_3 - E_2 M_B (2s_5 - s_7)}{\bar{u} (\bar{u} v k^2 - 2\bar{u} E_1 M_B - 2v E_2 M_B)} \right) \frac{\phi_{\pi}(v)}{v\bar{v}} \frac{\phi_B^+(\omega)}{\omega}, \quad (\text{B.34})$$

and

$$g_{(B3+B5)}^{\text{endpoint}} = C_{FA} \left( \frac{S_B^{(i)}(u) + S_B^{(ii)}(u)}{\bar{u}} \frac{\phi_{\pi}(v)}{v\bar{v}^2} \frac{\phi_B^-(\omega)}{\omega} - v_{\perp}^2 \frac{S_B^{(i)}(u)}{\bar{u}} \frac{\phi_{\pi}(v)}{\bar{v}^2} \frac{\phi_B^+(\omega)}{\omega} + v_{\perp}^2 \frac{S_B^{(i)}(u)}{\bar{u}} \frac{\mu_{\pi} \phi_{\sigma}(v)}{6E_2 \bar{v}^3} \frac{\phi_B^-(\omega)}{\omega} - v_{\perp}^2 \frac{S_B^{(i)}(u) + S_B^{(ii)}(u)}{\bar{u}} \frac{\mu_{\pi} \phi_{\sigma}(v)}{6E_2 \bar{v}^3} \frac{\phi_B^+(\omega)}{\omega} \right). \quad (\text{B.35})$$

### B.3.9 Diagram (B4)

$$g_{(B4)}^{\text{finite}} = C_{FA} \left( \frac{2E_2}{M_B} \left( \frac{2E_1 M_B}{k^2} - 1 \right) \frac{S_B^{(i)}(u)}{\bar{u}} - \frac{E_2}{M_B} \frac{s_3}{\bar{u}} \right) \frac{\phi_{\pi}(v)}{\bar{v}} \frac{\phi_B^+(\omega)}{\omega}, \quad (\text{B.36})$$

and

$$g_{(B4)}^{\text{endpoint}} = C_{FA} \left( \frac{2E_2 M_B}{k^2} \frac{s_5}{\bar{u}^2} \frac{\phi_{\pi}(v)}{\bar{v}} \frac{\phi_B^+(\omega)}{\omega} - \frac{S_B^{(i)}(u) + S_B^{(ii)}(u)}{\bar{u}} \frac{\phi_{\pi}(v)}{\bar{v}^2} \frac{\phi_B^-(\omega)}{\omega} + v_{\perp}^2 \frac{S_B^{(i)}(u)}{\bar{u}} \frac{\phi_{\pi}(v)}{\bar{v}^2} \frac{\phi_B^+(\omega)}{\omega} - v_{\perp}^2 \frac{S_B^{(i)}(u)}{\bar{u}} \frac{\mu_{\pi} \phi_{\sigma}(v)}{6E_2 \bar{v}^3} \frac{\phi_B^-(\omega)}{\omega} + v_{\perp}^2 \frac{S_B^{(i)}(u) + S_B^{(ii)}(u)}{\bar{u}} \frac{\mu_{\pi} \phi_{\sigma}(v)}{6E_2 \bar{v}^3} \frac{\phi_B^+(\omega)}{\omega} \right). \quad (\text{B.37})$$

### B.3.10 Diagram (B6)

$$g_{(B6)}^{\text{finite}} = C_A \left( \frac{S_B^{(i)}(u)}{\bar{u}} \left( \left( 1 - \frac{2E_2}{M_B} \right) \frac{\phi_{\pi}(v)}{2v} + v_{\perp}^2 \frac{\phi_{\pi}(v)}{2\bar{v}} \right) - \frac{E_2}{M_B} \frac{s_3}{\bar{u}} \frac{\phi_{\pi}(v)}{2v} \right) \frac{\phi_B^+(\omega)}{\omega}, \quad (\text{B.38})$$

and

$$g_{(B6)}^{\text{endpoint}} = C_A \left( \frac{2E_2 M_B}{k^2} \frac{s_5}{\bar{u}^2} \frac{(\bar{v} - v) \phi_{\pi}(v)}{4v\bar{v}} \frac{\phi_B^+(\omega)}{\omega} - \frac{S_B^{(i)}(u) + S_B^{(ii)}(u)}{\bar{u}} \frac{\phi_{\pi}(v)}{2v\bar{v}} \frac{\phi_B^-(\omega)}{\omega} \right). \quad (\text{B.39})$$

## C More on Kinematics

Expressing the energies  $E_{1,2}$  of the two pions in terms of the kinematic variables  $k^2, q^2, \cos \theta$ , one obtains

$$E_{1,2}(k^2, q^2, \cos \theta) = \frac{k^2 + M_B^2 - q^2 \pm \cos \theta \sqrt{\lambda(k^2, q^2)}}{4M_B}. \quad (\text{C.1})$$

Without loss of generality, we may assume that  $\cos \theta \geq 0$ , such that  $E_2 < E_1$ , and we thus have to determine the minimal value of  $E_2$  for given phase-space constraints on  $(k^2, q^2, \cos \theta)$ ,

$$E_{\min} = \min E_2(k^2, q^2, \cos \theta) \quad (\text{for } \cos \theta \geq 0). \quad (\text{C.2})$$

(For  $\cos \theta \leq 0$ , the same discussion goes through for  $E_1$ .) Since  $E_2$  is *decreasing* with  $\cos \theta$ , its minimal value (for fixed  $(k^2, q^2)$ ) is obtained for the maximal value  $\cos \theta|_{\max} \equiv 1/a$  with  $a \geq 1$ . Similarly,  $E_2$  is *increasing* with  $k^2$ , such that its minimal value is obtained for  $k^2 = k_{\min}^2$ . Concerning the  $q^2$ -dependence (for fixed values  $k^2 = k_{\min}^2$  and  $\cos \theta = 1/a$ ), the situation is more involved. The function  $E_2(q^2)$  exhibits a minimum at

$$q_{\star}^2 = M_B^2 + k_{\min}^2 - \frac{2aM_B\sqrt{k_{\min}^2}}{\sqrt{a^2 - 1}}. \quad (\text{C.3})$$

This always fulfills  $q_{\star}^2 \leq q_{\max}^2 = (M_B - \sqrt{k_{\min}^2})^2$ , which is the upper phase-space boundary for  $q^2$ . However, the condition  $q_{\star}^2 \geq 0$  yields a non-trivial relation between  $k_{\min}^2$  and  $a$ :

$$\text{minimum at } q_{\star}^2 \geq 0 \quad \Leftrightarrow \quad k_{\min}^2 \leq \frac{a-1}{a+1} M_B^2. \quad (\text{C.4})$$

We thus have to consider two cases

- $q_{\star}^2 \geq 0$ , with

$$\begin{aligned} E_{\min} &= E_2(k_{\min}^2, q_{\star}^2, 1/a) = \frac{\sqrt{a^2 - 1}}{2a} \sqrt{k_{\min}^2} \\ \Leftrightarrow \quad k_{\min}^2 &= \frac{4a^2}{a^2 - 1} E_{\min}^2, \end{aligned} \quad (\text{C.5})$$

for which the relation (C.4) translates into (using  $E_2 \leq M_B/2$ )

$$E_{\min} < \frac{a-1}{a} \frac{M_B}{2}. \quad (\text{C.6})$$

- $q_{\star}^2 < 0$ , with

$$\begin{aligned} E_{\min} &= E_2(k_{\min}^2, 0, 1/a) = \frac{(a+1)k^2 + (a-1)M_B^2}{4aM_B} \\ \Leftrightarrow \quad k_{\min}^2 &= \frac{4aM_B E_{\min} - (a-1)M_B^2}{a+1} \end{aligned} \quad (\text{C.7})$$

for which the complement of the relation (C.4) now consistently translates into

$$E_{\min} > \frac{a-1}{a} \frac{M_B}{2}. \quad (\text{C.8})$$

Notice that (C.7) always holds for  $a = 1$ , in which case the minimal value of  $E_2$  is given at  $q^2 = 0$ , and  $k_{\min}^2 = 2M_B E_{\min}$ , as in Scenarios A and B defined in the text. For a given value of  $E_{\min}$ , there is a critical value of the angular cut,  $a_* = M_B/(M_B - 2E_{\min})$ , above which (C.5) is to be used. In our Scenario C we took  $k_{\min}^2 = M_B^2/4$  and  $a = 3$ , for which one actually has  $q_*^2 > 0$ , and therefore the correct expression for  $k_{\min}^2$  reads

$$\begin{aligned} k_{\min}^2 &= M_B^2/4, \quad |\cos \theta| \leq 1/3 \\ \Rightarrow E_{\min} &= \frac{\sqrt{a^2 - 1}}{2a} \sqrt{k_{\min}^2} = \frac{1}{3\sqrt{2}} M_B \simeq 1.24 \text{ GeV}. \end{aligned} \quad (\text{C.9})$$

(For the resulting value of  $E_{\min}$  one has  $a_* \simeq 1.89$ , and therefore  $a > a_*$  in our Scenario C.)

## References

- [1] M. Artuso et al., *B, D and K decays*, *Eur. Phys. J.* **C57** (2008) 309–492, [[0801.1833](#)].
- [2] M. Antonelli et al., *Flavor Physics in the Quark Sector*, *Phys. Rept.* **494** (2010) 197–414, [[0907.5386](#)].
- [3] LHCb collaboration, R. Aaij et al., *Implications of LHCb measurements and future prospects*, *Eur. Phys. J.* **C73** (2013) 2373, [[1208.3355](#)].
- [4] A. J. Buras and J. Girrbach, *Towards the Identification of New Physics through Quark Flavour Violating Processes*, *Rept. Prog. Phys.* **77** (2014) 086201, [[1306.3775](#)].
- [5] BELLE, BABAR collaboration, A. J. Bevan et al., *The Physics of the B Factories*, *Eur. Phys. J.* **C74** (2014) 3026, [[1406.6311](#)].
- [6] M. Beneke, G. Buchalla, M. Neubert and C. T. Sachrajda, *QCD factorization for  $B \rightarrow \pi\pi$  decays: Strong phases and CP violation in the heavy quark limit*, *Phys.Rev.Lett.* **83** (1999) 1914–1917, [[hep-ph/9905312](#)].
- [7] M. Beneke, G. Buchalla, M. Neubert and C. T. Sachrajda, *QCD factorization in  $B \rightarrow \pi K, \pi\pi$  decays and extraction of Wolfenstein parameters*, *Nucl.Phys.* **B606** (2001) 245–321, [[hep-ph/0104110](#)].
- [8] G. Bell, *NNLO vertex corrections in charmless hadronic B decays: Imaginary part*, *Nucl. Phys.* **B795** (2008) 1–26, [[0705.3127](#)].
- [9] G. Bell, *NNLO vertex corrections in charmless hadronic B decays: Real part*, *Nucl. Phys.* **B822** (2009) 172–200, [[0902.1915](#)].
- [10] M. Beneke, T. Huber and X.-Q. Li, *NNLO vertex corrections to non-leptonic B decays: Tree amplitudes*, *Nucl. Phys.* **B832** (2010) 109–151, [[0911.3655](#)].
- [11] G. Bell, M. Beneke, T. Huber and X.-Q. Li, *Two-loop current-current operator contribution to the non-leptonic QCD penguin amplitude*, *Phys. Lett.* **B750** (2015) 348–355, [[1507.03700](#)].
- [12] M. Beneke and S. Jäger, *Spectator scattering at NLO in non-leptonic b decays: Tree amplitudes*, *Nucl. Phys.* **B751** (2006) 160–185, [[hep-ph/0512351](#)].
- [13] N. Kivel, *Radiative corrections to hard spectator scattering in  $B \rightarrow \pi\pi$  decays*, *JHEP* **05** (2007) 019, [[hep-ph/0608291](#)].
- [14] V. Pilipp, *Hard spectator interactions in  $B \rightarrow \pi\pi$  at order  $\alpha_s^2$* , *Nucl. Phys.* **B794** (2008) 154–188, [[0709.3214](#)].

- [15] M. Beneke and S. Jäger, *Spectator scattering at NLO in non-leptonic B decays: Leading penguin amplitudes*, *Nucl. Phys.* **B768** (2007) 51–84, [[hep-ph/0610322](#)].
- [16] T. Feldmann, *Non-Leptonic Heavy Meson Decays - Theory Status*, in *12th Conference on Flavor Physics and CP Violation (FPCP 2014) Marseille, France, May 26-30, 2014*, 2014. [1408.0300](#).
- [17] M. Beneke and M. Neubert, *QCD factorization for  $B \rightarrow PP$  and  $B \rightarrow PV$  decays*, *Nucl. Phys.* **B675** (2003) 333–415, [[hep-ph/0308039](#)].
- [18] M. Beneke, J. Rohrer and D. Yang, *Branching fractions, polarisation and asymmetries of  $B \rightarrow VV$  decays*, *Nucl. Phys.* **B774** (2007) 64–101, [[hep-ph/0612290](#)].
- [19] H.-n. Li, S. Mishima and A. I. Sanda, *Resolution to the  $B \rightarrow \pi K$  puzzle*, *Phys. Rev.* **D72** (2005) 114005, [[hep-ph/0508041](#)].
- [20] H.-Y. Cheng, C.-K. Chua and A. Soni, *Final state interactions in hadronic B decays*, *Phys. Rev.* **D71** (2005) 014030, [[hep-ph/0409317](#)].
- [21] C. W. Bauer, I. Z. Rothstein and I. W. Stewart, *SCET analysis of  $B \rightarrow K\pi$ ,  $B \rightarrow K\bar{K}$ , and  $B \rightarrow \pi\pi$  decays*, *Phys. Rev.* **D74** (2006) 034010, [[hep-ph/0510241](#)].
- [22] T. Feldmann, M. Jung and T. Mannel, *Is there a non-Standard-Model contribution in non-leptonic  $b \rightarrow s$  decays?*, *JHEP* **08** (2008) 066, [[0803.3729](#)].
- [23] G. Bell and V. Pilipp,  *$B^- \rightarrow \pi^- \pi^0 / \rho^- \rho^0$  to NNLO in QCD factorization*, *Phys. Rev.* **D80** (2009) 054024, [[0907.1016](#)].
- [24] M. Beneke and T. Feldmann, *Symmetry breaking corrections to heavy to light B meson form-factors at large recoil*, *Nucl. Phys.* **B592** (2001) 3–34, [[hep-ph/0008255](#)].
- [25] C. W. Bauer, S. Fleming, D. Pirjol and I. W. Stewart, *An Effective field theory for collinear and soft gluons: Heavy to light decays*, *Phys. Rev.* **D63** (2001) 114020, [[hep-ph/0011336](#)].
- [26] M. Beneke, A. P. Chapovsky, M. Diehl and T. Feldmann, *Soft collinear effective theory and heavy to light currents beyond leading power*, *Nucl. Phys.* **B643** (2002) 431–476, [[hep-ph/0206152](#)].
- [27] M. Beneke and T. Feldmann, *Factorization of heavy to light form-factors in soft collinear effective theory*, *Nucl. Phys.* **B685** (2004) 249–296, [[hep-ph/0311335](#)].
- [28] M. Beneke and T. Feldmann, *Spectator interactions and factorization in  $B \rightarrow \pi \ell \nu$  decay*, *Eur. Phys. J.* **C33** (2004) S241–S243, [[hep-ph/0308303](#)].
- [29] F. Krüger and J. Matias, *Probing new physics via the transverse amplitudes of  $B^0 \rightarrow K^{*0}(\rightarrow K^- \pi^+) \ell^+ \ell^-$  at large recoil*, *Phys. Rev.* **D71** (2005) 094009, [[hep-ph/0502060](#)].
- [30] W. Altmannshofer, P. Ball, A. Bharucha, A. J. Buras, D. M. Straub and M. Wick, *Symmetries and Asymmetries of  $B \rightarrow K^* \mu^+ \mu^-$  Decays in the Standard Model and Beyond*, *JHEP* **01** (2009) 019, [[0811.1214](#)].
- [31] C. Bobeth, G. Hiller and D. van Dyk, *The Benefits of  $\bar{B} \rightarrow \bar{K}^* l^+ l^-$  Decays at Low Recoil*, *JHEP* **07** (2010) 098, [[1006.5013](#)].
- [32] T. Feldmann, B. Müller and D. van Dyk, *Analyzing  $b \rightarrow u$  transitions in semileptonic  $\bar{B}_s \rightarrow K^{*+}(\rightarrow K\pi) \ell^- \bar{\nu}_\ell$  decays*, *Phys. Rev.* **D92** (2015) 034013, [[1503.09063](#)].
- [33] U.-G. Meißner and W. Wang,  *$B_s \rightarrow K^{(*)} \ell \bar{\nu}$ , Angular Analysis, S-wave Contributions and  $|\mathbf{V}_{ub}|$* , *JHEP* **01** (2014) 107, [[1311.5420](#)].

- [34] P. Böer, T. Feldmann and D. van Dyk, *Angular Analysis of the Decay  $\Lambda_b \rightarrow \Lambda(\rightarrow N\pi)\ell^+\ell^-$* , *JHEP* **01** (2015) 155, [[1410.2115](#)].
- [35] S. Faller, T. Feldmann, A. Khodjamirian, T. Mannel and D. van Dyk, *Disentangling the Decay Observables in  $B^- \rightarrow \pi^+\pi^-\ell^-\bar{\nu}_\ell$* , *Phys. Rev.* **D89** (2014) 014015, [[1310.6660](#)].
- [36] X.-W. Kang, B. Kubis, C. Hanhart and U.-G. Meißner,  *$B_{l4}$  decays and the extraction of  $|V_{ub}|$* , *Phys. Rev.* **D89** (2014) 053015, [[1312.1193](#)].
- [37] U.-G. Meißner and W. Wang, *Generalized Heavy-to-Light Form Factors in Light-Cone Sum Rules*, *Phys. Lett.* **B730** (2014) 336–341, [[1312.3087](#)].
- [38] C. Hambrock and A. Khodjamirian, *Form factors in  $\bar{B}^0 \rightarrow \pi\pi\ell\bar{\nu}_\ell$  from QCD light-cone sum rules*, *Nucl. Phys.* **B905** (2016) 373–390, [[1511.02509](#)].
- [39] S. Kränkl, T. Mannel and J. Virto, *Three-Body Non-Leptonic B Decays and QCD Factorization*, *Nucl. Phys.* **B899** (2015) 247–264, [[1505.04111](#)].
- [40] V. M. Braun and I. E. Filyanov, *Conformal Invariance and Pion Wave Functions of Nonleading Twist*, *Z. Phys.* **C48** (1990) 239–248.
- [41] G. Hiller and R. Zwicky, *(A)symmetries of weak decays at and near the kinematic endpoint*, *JHEP* **1403** (2014) 042, [[1312.1923](#)].
- [42] PARTICLE DATA GROUP collaboration, J. Beringer et al., *Review of Particle Physics (RPP)*, *Phys. Rev.* **D86** (2012) 010001.
- [43] I. Sentitemsu Imsong, A. Khodjamirian, T. Mannel and D. van Dyk, *Extrapolation and unitarity bounds for the  $B \rightarrow \pi$  form factor*, *JHEP* **02** (2015) 126, [[1409.7816](#)].
- [44] A. Khodjamirian, T. Mannel, N. Offen and Y. M. Wang,  *$B \rightarrow \pi\ell\nu_l$  Width and  $|V_{ub}|$  from QCD Light-Cone Sum Rules*, *Phys. Rev.* **D83** (2011) 094031, [[1103.2655](#)].
- [45] D. van Dyk et al., *EOS – A HEP Program for Flavour Observables*, 2016. DOI: [10.5281/zenodo.60884](#), see also the release at <https://github.com/eos/eos/releases/tag/btopipilnu-qcdf>.
- [46] A. Bharucha, T. Feldmann and M. Wick, *Theoretical and Phenomenological Constraints on Form Factors for Radiative and Semi-Leptonic B-Meson Decays*, *JHEP* **09** (2010) 090, [[1004.3249](#)].
- [47] T. Feldmann and M. W. Y. Yip, *Form Factors for  $\Lambda_b \rightarrow \Lambda$  Transitions in SCET*, *Phys. Rev.* **D85** (2012) 014035, [[1111.1844](#)].
- [48] D. Das and R. Sinha, *New Physics Effects and Hadronic Form Factor Uncertainties in  $B \rightarrow K^*\ell^+\ell^-$* , *Phys. Rev.* **D86** (2012) 056006, [[1205.1438](#)].
- [49] C. Hambrock and G. Hiller, *Extracting  $B \rightarrow K^*$  Form Factors from Data*, *Phys. Rev. Lett.* **109** (2012) 091802, [[1204.4444](#)].